

DEVELOPMENT OF AN EEG-BASED ARM EXOSKELETON ROBOT

by

Sunny Raj Shrestha

A Thesis Submitted in Partial Fulfillment of the Requirements for the Degree of
Master of Engineering in Mechatronics

Examination Committee: Prof. Manukid Parnichkun (Chairperson)
Dr. Mongkol Ekpanyapong
Dr. Tanujjal Bora

Nationality: Nepali
Previous Degree: Bachelor of Engineering in Computing
(Computer Network Engineering)
University of Northampton
Northampton, UK

Scholarship Donor: AIT Scholarships

Asian Institute of Technology
School of Engineering and Technology
Thailand
May 2024

AUTHOR'S DECLARATION

I, Sunny Raj Shrestha, declare that the research work carried out for this thesis was in accordance with the regulations of the Asian Institute of Technology. The work presented in it are my own and has been generated by me as the result of my own original research, and if external sources were used, such sources have been cited. It is original and has not been submitted to any other institution to obtain another degree or qualification. This is a true copy of the thesis, including final revisions.

Date: 6 May 2024

Name (in printed letters): Sunny Raj Shrestha

Signature:

A handwritten signature in black ink, consisting of a stylized 'S' followed by a diagonal line.

ACKNOWLEDGMENTS

I would like to thank my parents for supporting my dream of studying mechatronics and always being the strongest pillars of my life. I would like to thank my Professor, Prof. Manukid Parnichkun for always supporting me and guiding me throughout my master's journey.

I would like to thank my late grandmother, Karuna Laxmi Tuladhar for always encouraging and inspiring me to pursue creating technology and innovation that starts with having a compassionate and curious heart as hers.

I would not have made it without my dear friends, Xavier, Changrui, Supakorn, Ania, Thongtong. Moreover, I really learnt a lot from my seniors, Khun Matee, Khun Sudarat, Khun Yasiru and I am also grateful for their motivation and support throughout.

Moreover, I would also like to thank our lab supervisor, Mr. Manh and Khun Thanit, Program secretaries, Khun Parin, Khun Chowaret, Khun Saowaluck Maneerat for their constant and everlasting care and guidance.

ABSTRACT

Robotics in terms of Brain-Machine Interface is the union between a human mind and a robot or computer, which gives the human being a new technological evolution to make their lives easy, happy and overall better. This paper presents Karuna Robot, which is a 2 Degrees of freedom arm exoskeleton rehabilitation robot that picks and places an object following the commands of the EEG signals to study about the effectiveness and possibilities of recovery of motor movements by using a non-invasive motor imagery technique. The EEG headset is a 5 channel Emotiv Insight 2.0 headset that facilitates effective communication between the user and the robot to execute the task of pick-and-place using combinations of mental commands to move the two joints of Karuna Robot which performs grasping and releasing the object at desired positions. The Average Root Mean Square Error of the joints in both positive and negative directions is 14.86 degrees, whereas, the signal band power analysis renders prominence of Theta, Alpha and a very few spikes of low beta waves during the window of mental commands which illustrates presence of recall of memory, motor planning and active thinking, respectively. Moreover, the circular queue data structure and the use of linear interpolation has also rendered optimized and nuanced user-controlled movements. The average time for the pick-and-place task completion is about 2 minutes, with time complexity of $O(1)$ and a success rate of about 70%.

Keywords: Brain Machine Interface, Exoskeleton arm Robot, Rehabilitation device, signal processing.

CONTENTS

	Page
AUTHOR'S DECLARATION	ii
ACKNOWLEDGEMENTS	iii
ABSTRACT	iv
LIST OF TABLES	vii
LIST OF FIGURES	viii
CHAPTER 1 INTRODUCTION	1
1.1 Background of the Study	1
1.2 Statement of the Problem	2
1.3 Objectives of the Research	2
1.4 Contributions	3
1.5 Limitations and Scope	3
1.5.1 Limitations	3
1.5.2 Scopes	
CHAPTER 2 LITERATURE REVIEW	4
2.1 Exoskeleton Robot	4
2.1.1 EEG Signals	6
2.1.2 Mixed Bio-signals	11
2.2 Soft Exoskeleton Actuators	13
2.2.1 Cable Actuation	13
2.2.2 Pneumatic Actuators	14
2.3 Control	15
2.3.1 Impedance and Admittance Control	16
2.3.2 Adaptive Control	17
2.3.3 Position Control	18
CHAPTER 3 METHODOLOGY	20
3.1 Overview of System	20
3.1.1 System Controllers	22
3.2 Mechanical Design	24
3.3 Data Structure: Circular Queue and Linear Interpolation	27
3.4 Brain Machine Interface System	30

3.4.1 Experimental Setup	32
3.4.2 Signal Collection and Pre-Processing	33
CHAPTER 4 RESULTS	38
4.1 Control Degree of Movement	38
4.2 Pick and Place	53
4.3 Signals Average Band Power	57
CHAPTER 5 CONCLUSION	62
5.1 Summary	62
5.2 Future Works	63
REFERENCES	64

LIST OF TABLES

Tables	Page
Table 3.1 EEG Electrodes and their Meaning	31
Table 4.1 Joint 1: 30 Degrees Movement from 90	39
Table 4.2 Joint 1:180 Degree Movement from 90	42
Table 4.3 Joint 2: 45 Degree Movement from 90	45
Table 4.4 Joint 2: 180 Degree Movement from 90	49
Table 4.5 Ten Trials of Pick and Place	55
Table 4.6 Average Signal Band Power	57

LIST OF FIGURES

Figures	Page
Figure 2.1 Rehabilitation Upper Limb Exoskeletons.	4
Figure 2.2 Dh Parameter of Upper Limb.	5
Figure 2.3 Different Brain Frequencies and their Associations	6
Figure 2.4 5 Channels EMOTIV Insight 2.0 EEG Headset.	7
Figure 2.5 A Brain Machine Interface Control	8
Figure 2.6 Gaussian Model to Render the Intensity of Thoughts.	8
Figure 2.7 Emotiv EEG Headset and GUI	9
Figure 2.8 Thought Intensity	10
Figure 2.9 Gaussian Model for Intensity of the Thoughts	10
Figure 2.10 Upper Limb Exoskeleton Multi-Sensing and Feedback.	11
Figure 2.11 EMG and Force Sensors with Bowden Cables	12
Figure 2.12 Upper Limb Soft Exoskeletons and Types of Actuators	13
Figure 2.13 A 3D Model of the Bowden Actuation	14
Figure 2.14 18 Weaves McKibben Muscle	15
Figure 2.15 Impedance and Admittance Control (EduExo,2023)	16
Figure 2.16 2 DOF Exoskeleton with Impedance Control	17
Figure 2.17 Control Techniques with Non-Bio Sensor Feedback	18
Figure 2.18 Position Control Block Diagram	19
Figure 3.1 System Overview Block	20
Figure 3.2 Flowchart of the Working of the System	21
Figure 3.3 Emotiv Insight 2 Headset	22
Figure 3.4 Arduino Mega Micro-Controller	23
Figure 3.5 Design of Karuna Robot	24
Figure 3.6 Motor Housing	24
Figure 3.7 Motor Interface	25
Figure 3.8 Link	25
Figure 3.9 Cuffs (2)	26
Figure 3.10 Motor Housing	26

Figure 3.11 Gripper (Open-Source Gripper on Grabcad Website (Anand, 2023)	27
Figure 3.12 Enqueue Method for Mental Commands.	28
Figure 3.13 Complete Mechanical Design of Karuna Robot	29
Figure 3.14 5 Channel EEG Headset: Emotiv Insight 2 (Hendradi, 2018)	30
Figure 3.15 Training Mental Commands	32
Figure 3.16 Feedbacks Box for Mental Commands	33
Figure 3.17 Raw EEG Data Recording	34
Figure 3.18 Raw EEG Data to .CSV Files in Time Series	35
Figure 3.19 Preprocessed EEG Data in Frequency Domain	36
Figure 3.20 Mental Commands Trigger Time Stamps	37
Figure 4.1 MAE and RMSE Formula (Acharya, 2021)	38
Figure 4.2 Exoskeleton Robot Joint 1: 30 Degrees from 90	40
Figure 4.3 Joint 1: 30 Degrees from 90 Graph	41
Figure 4.4 Joint 1 Attempt to Move to 180 Degrees	43
Figure 4.5 Joint 1 180 Degrees Graph	44
Figure 4.6 Joint 2 45 Degrees Movement	46
Figure 4.7 Joint 2 45 Degrees Movement Graph	47
Figure 4.8 Joint 2 45 Degrees Movement	48
Figure 4.9 Joint 2 180 Degree from 90	50
Figure 4.10 Average MAE in Both Joints.	51
Figure 4.11 Average RMSE Across All Joints and Directions	52
Figure 4.12 Pick and Place Set Up	53
Figure 4.13 Place Operation from One Point to Another	54
Figure 4.14 Pick and Place Success Rate	56
Figure 4.15 Neutral State	58
Figure 4.16 Push State Compared with Baseline	59
Figure 4.17 Pull State Compared with Baseline	60
Figure 4.18 Lift state Compared with Baseline	61

CHAPTER 1

INTRODUCTION

1.1 Background of the Study

In the modern era, robotics is not only implemented widely in an industrial setup because of its speed and accuracy of performing repetitive, dangerous and difficult tasks for an ordinary human but it is also used extensively in the medical sector; especially in the rehabilitation of patients who lack motor functions and are deprived of using their arms or legs, either for a short time or perhaps permanently due to some physical conditions like stroke which accounts for about 15 million patients every year and out of which 5 million are rendered permanently disabled (Benesová et al., 2022) like paralysis and or impairment of vision and speech etc.

Robots aid in the improvement or and recovery of motor functions in patients diagnosed with stroke (Zhu et al., 2020). Karuna Robot is a 2 degrees of freedom arm exoskeleton robot that uses Motor imagery as it leverages upon the imagination of the movements of hands and legs from the user without really making any actual physical movement (Arpaia et al., 2022) and uses the same signals from brain using Electroencephalography (EEG) based interface which further lets them interact with the karuna robot to pick and place an object. Thus, having potential to train the brain to produce neuroplasticity which helps to rewire motor function to render in the recovery and reinstate neurophysiological functions (Qu et al., 2022). However, this is possible as long as the patient still has a normal functioning brain which is still capable of making motor-based neural activities (McFarland & Wolpaw., 2011).

Various techniques have been researched to collect neurophysiological signals from the brain and there are two ways to do this, namely, invasive, partially invasive and noninvasive BCI based on the level of how close the electrodes are from the brain tissues (Gupta et al., 2018) (Martini et al., 2020). The Invasive BCI use a more directly implanted microelectrode in the cortex to record neurophysiological signals which has better performance than non-invasive method in terms of higher spatial resolution and better signal to noise ratio. However, Karuna robot uses non-invasive BCI, which is much safer, economical and easier to use. Thus, Electroencephalography (EEG) is the data that is taken using non-invasive BCI, which is used to capture brain activities and signals by putting the electrodes on the scalp of the subject (Abdulkader et al., 2015).

In the current scenario, BMI/BCI technology is being used to control many machines and robots like exoskeleton, quadcopters, wheelchairs, virtual cursors. Researches are being conducted to rehabilitate patients with neurological disorder to control robotic arm to conduct grabbing objects. However, robotics in the field of rehabilitation of stroke patients using Motor imagery and brain computer interface is a novel and advanced technique in its infancy (Chen et al., 2022) because as the Degree of Freedom (DOF) increases in robotic arms, the more complex it is to hold on to multiple objects in a 3D space, persistently and successfully (Xu et al., 2022).

The details regarding Karuna robot's design is given in chapter 3 which describes the mechanical and the pick and place rehabilitation design, data structure to optimize the time complexity of pick and place and all the signal processing for the raw EEG data is given sequentially. Moreover, the test results for control of degree of movement, calculations of band power and errors and overall success rate of pick and place is given in chapter 4.

1.2 Statement of the Problem

In the field of rehabilitation, the patients usually have either low or absolutely no motor movement. Thus, exoskeleton robots can provide some gait restoration. However, exoskeleton is depended on how the user interfaces with it too. It takes into consideration of the movement intention of the user. However, some user may have no control of their arm movement which can be facilitated with EEG command as a high-level control strategy to let the actuators and sensors perform a recorded movement with regard to the intentions on the patient. Decoding EEG signal to get the real time motor intention of the user is difficult.

1.3 Objectives of the Research

The objective of this paper is to create an exoskeleton arm robot, Karuna, to pick and place object with EEG Signals.

1. A Brain machine interface system with an exoskeleton arm robot.
2. Create a pick and place system.
3. Manage, structure and organize the EEG signals to have desired control movements.
4. Analyze Signal processing of raw EEG data (offline).

1.4 Contributions

The contributions in the research are as follows:

- Circular Queue Data Structure to manage and optimize the commands from EEG signals.
- Design of a custom linear interpolation function to resonate EEG signal power with the degree of joint movements rather than binary movements or just have absolute positive or negative movements.

1.5 Limitations and Scope

1.5.1 Limitations

The online raw EEG data could not be acquired due to student license limitations for the Emotiv Insight 2.0 headset. The raw EEG data is recorded, only then the signal is pre-processed and analyzed. Thus, Online and real time classification and modification of algorithms to classify patterns of EEG data is the only step the paper was not able to carry out.

1.5.2 Scopes

1. Create 2 Degree of Freedom Robot
2. Torque of servo is 3.4 Nm.
3. Length and fitting suitable for average Asian arm.
4. Pick and place.

CHAPTER 2

LITERATURE REVIEW

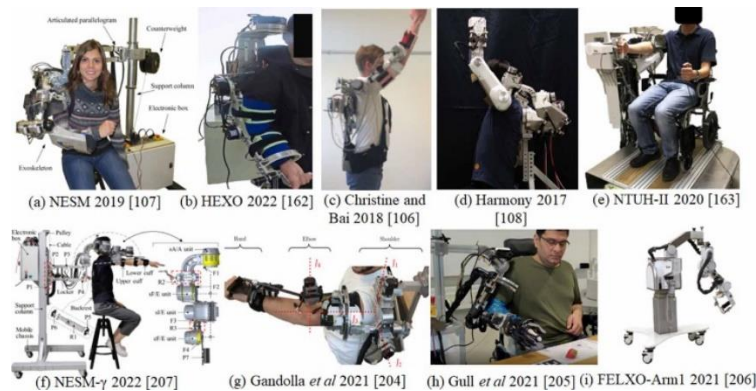
Controlling an exoskeleton robot arm with the signals from brain which intends to make motor movements for rehabilitation is the main purpose of this study. The brain machine interface based on motor imagery signals to control an exoskeleton arm is proposed. The literature discusses the following topics:

2.1 Exoskeleton Robot

An exoskeleton robot or wearable robot is defined as “powered devices that attach around and to a human or animal body and contain actuators that deliver mechanical power to aid movement. (Ferris et al., 2019). Recently, more wearable, portable, and lightweight exoskeletons are being developed, enabling broader healthcare applications as shown in Figure 2.1.

Figure 2.1

Rehabilitation Upper Limb Exoskeletons.



There are namely two types of robots used as assistive robots for rehabilitation and Activities of Daily Living (ADL): end effector-based systems and wearable exoskeletons. End effector robots apply forces and guide the hand for therapy but doesn't render information about joint angles of humans (β_i) as shown in Figure 2.2. Wearable exoskeletons enhance mobility and control human joints, providing multiple degrees of freedom, but are complex to design.

Figure 2.2*Dh Parameter of Upper Limb.*

Joint	Physiological ROM of β_i	i	α_i	a_i	d_i	θ_i
Base	Zero	$1_{(0 \rightarrow 1)}$	0	a_0	d_0	0
Shoulder	Internal rotation (-90°), external rotation ($+90^\circ$)	$2_{(1 \rightarrow 2)}$	-90°	0	0	$\beta_1 + 90^\circ$
Shoulder	Abduction (-180°), adduction ($+50^\circ$)	$3_{(2 \rightarrow 3)}$	$+90^\circ$	0	0	$\beta_2 + 90^\circ$
Shoulder	Flexion (-180°), extension ($+80^\circ$)	$4_{(3 \rightarrow 4)}$	0	l_u	0	$\beta_3 + 90^\circ$
Elbow	Extension (-10°), flexion ($+145^\circ$)	$5_{(4 \rightarrow 5)}$	$+90^\circ$	0	0	$\beta_4 + 90^\circ$
Elbow	Pronation (-90°), supination ($+90^\circ$)	$6_{(5 \rightarrow 6)}$	$+90^\circ$	0	l_f	$\beta_5 + 90^\circ$
Wrist	Flexion (-90°), extension ($+70^\circ$)	$7_{(6 \rightarrow 7)}$	$+90^\circ$	0	0	$\beta_6 + 90^\circ$
Wrist	Abduction (-15°), adduction ($+40^\circ$)	$8_{(7 \rightarrow 8)}$	0	l_h	0	β_7

According to the intended use, aspects like degrees of freedom (DOF), sensing and control techniques, actuators, power transfer, and the particular upper limb segment to be controlled must be taken into account while constructing upper-limb exoskeletons. Planned joint motions and motion trajectories are the main emphasis of rehabilitation robots.

Exoskeletons for rehabilitation should deliver routine, task-focused care with customizable controller designs based on patient individualization and rehabilitation stages. Depending on the patient's muscle control status, control tactics might be either patient-passive or patient-cooperative. In order to improve human-robot interaction for better care, motion intention estimate is essential. There are some bio signals that can be used, such as:

2.1.1 EEG Signals

EEG is induced by the neurons that fire electrical signal in the brain. These are categorized as per the frequency they produce, such as the delta, alpha, beta and gamma. When a person does an activity like extension of arm, they create Event-related desynchronization signals that the electrodes in EEG caps can detect and use this very signal as an input to a computer or robot Esposito et al. (2021). There are two types of EEG, namely, invasive and non-invasive. While Invasive methods for a Brain machine Interface is being developed by Elon Musk, CEO of Neuralink Musk. (2019) which has been granted approval for the first human trial by The US FDA for the same. Paul & Singh. (2023). However, the most commonly used method for BMI is Non-invasive.

Figure 2.3

Different Brain Frequencies and Their Associations

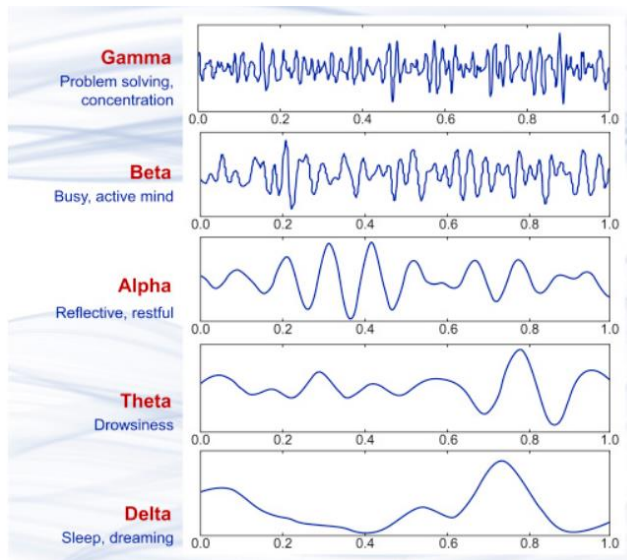
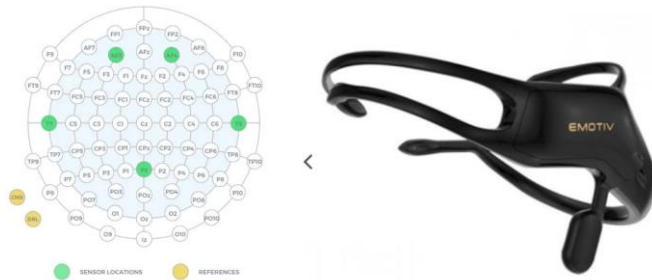


Figure 2.4

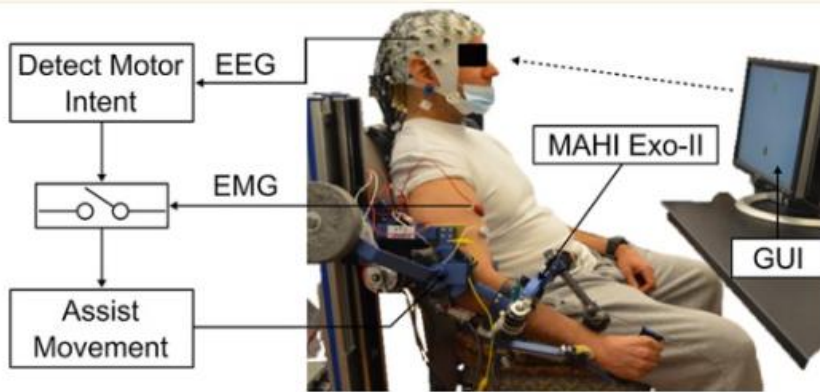
5 Channels EMOTIV Insight 2.0 EEG Headset.



The authors in Bhagat et al. (2016) presented MAHI Exo II, which used EEG signals to control an upper limb 4 DOF exoskeleton arm for a stroke patient. They assess the feasibility of an EEG-based brain-machine interface (BMI) for detecting motor intent in chronic stroke patients. MRCPs (movement related cortical potentials) measured by EEG electrodes drove an upper-limb exoskeleton for guided movement. BMI optimizations included adaptive time windows, pooling training data from consecutive days, and gating predictions with residual EMG to reduce false positives. The patient-specific BMI calibration accommodated diverse stroke patients. Testing showed consistent BMI performance across multiple days without recalibration, with a mean TPR (total positive rate) of $62.7 \pm 21.4\%$ on day 4 and $67.1 \pm 14.6\%$ on day 5. The FPR varied across subjects but remained low for those with residual motor function. On average, motor intent was detected approximately 367 ± 328 ms before movement onset during closed-loop operation. These findings highlight the potential for a robust, closed-loop EEG-based BMI for stroke patients without frequent recalibration. Despite all this, the system had lots of signal noise which created some hindrance in using the MRCPs.

Figure 2.5

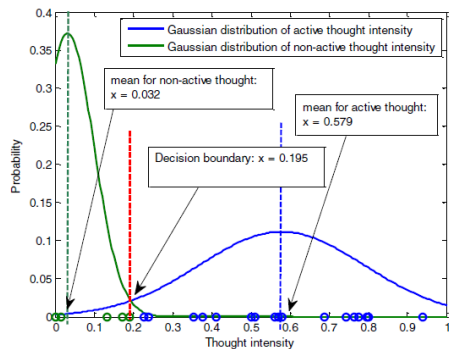
A Brain Machine Interface Control



Xiao. (2014) designed an exoskeleton arm with 4 DOF by using an Emotiv EEG headset with The Emotiv EEG headset that has 14 electrodes, which are located at AF3, F7, F3, FC5, T7, P7, O1, O2, P8, T8, FC6, F4, F8, and AF4 according to the International 10-20 system. The users were trained on the Emotiv's application software to imagine moving cubes as shown in Figure 2.7 Since the thoughts were not very consistent, they averaged the time for a movement to take place and only when the thought is consistent and waits 3 seconds to execute the mental commands. A good combination of timing for executing, thinking and resting were taken to fine tune movements imagined by the user. Gaussian classifier as shown in Figure 2.6, was used in order to state the optimum decision boundary of thoughts.

Figure 2.6

Gaussian Model to Render the Intensity of Thoughts.



However, it only holds true for one volunteer. It is still not a generalized system which will work to seamlessly use EEG signals to move every movement accurately. Moreover, EEG and exoskeletons have been used for rehabilitation, but it is still in a very preliminary stage as the difficulty lies in decoding the neural activity correctly and also the signal processing classification. EEG signals might be a better solution to the already existing EMG based control with a high signal to noise ratio along with almost no training required but as patients suffering from stroke might have muscle atrophy and may have lost muscle signals already. In such cases EEG signals from brain can be used to rewire (neuroplasticity) the patient's brain to use the motor movements again, despite the noise and variability in the signal.

Figure 2.7

Emotiv EEG Headset and GUI



Figure 2.8

Thought Intensity

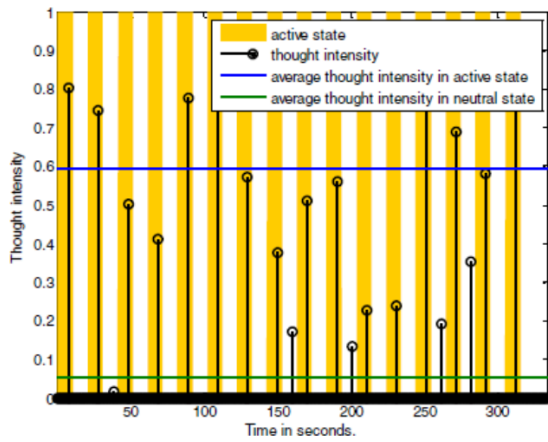
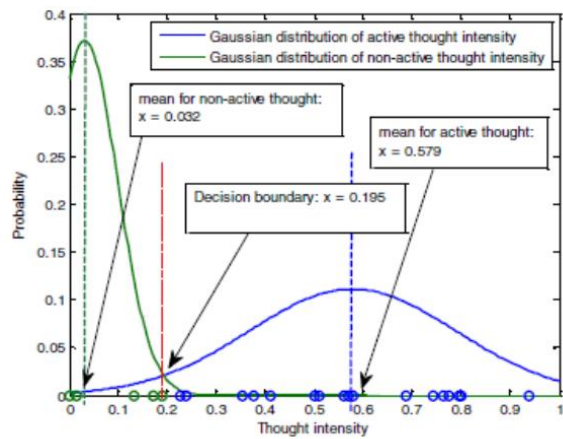


Figure 2.9

Gaussian Model for Intensity of the Thoughts

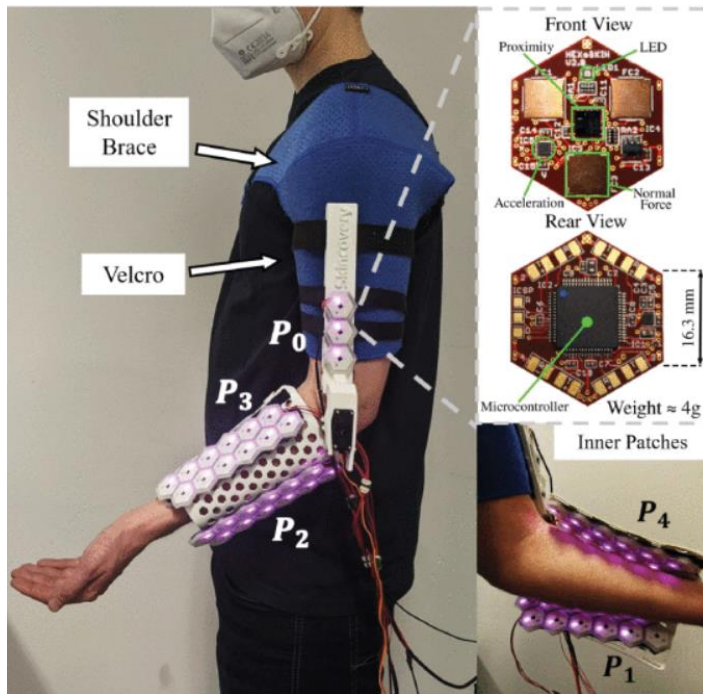


2.1.2 Mixed Bio-signals

The Figure 2.10 renders exoskeleton arm with mixed bio-signals and electronics sensors.

Figure 2.10

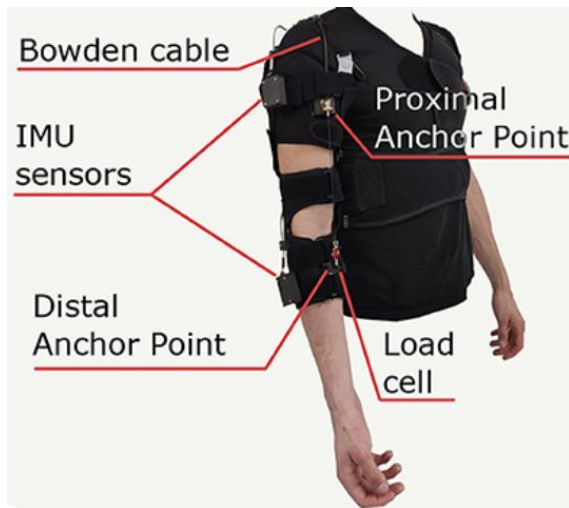
Upper Limb Exoskeleton Multi-Sensing and Feedback.



Paredes-Acuna et al. (2022) present a lightweight 3D printed exoskeleton built for elbow flexion/extension that uses a robot skin to detect motion intention via acceleration, proximity, and interface forces. The exoskeleton integrates physical therapy-inspired control modes such as passive mobility, active support, resistance training, and corrective treatment. To examine the functionality of the exoskeleton, the researchers conducted a study with four healthy volunteers, analyzing force readings and sEMG recordings of the biceps during exoskeleton use. Higher assistive levels in supportive therapy modes resulted in significant decreases in normalized sEMG (over 40% in passive exercises), whereas higher resistive levels resulted in increases in normalized sEMG (over 30% in resistive exercises). This shows that the exoskeleton can alter therapeutic regimens based on user intent via multi-sensory interfaces. However, the paper does not cover any experiments where the user with very less to no movement due to muscle atrophy even though the paper tries to use multiple bio and non-bio sensing.

Figure 2.11

EMG and Force Sensors with Bowden Cables



Missiroli et al. (2020) in their study investigated the impact of assistance magnitude on human performance using a myoelectric-driven exoskeleton suit. Findings revealed consistent advantages in terms of muscular activation magnitude and delayed onset of fatigue with increasing assistive levels. Importantly, the inclusion of muscular activity in the control loop did not compromise movement smoothness as assistive magnitude increased. The results indicate that the combination of the hardware and control frameworks is reliable for detecting movement intention and adapting real-time assistance. The research does not take into consideration about the noise and muscle fatigue.

It is mostly the combination of using both EMG and EEG signals to render an interface between robots and humans. Lalitharatne and colleagues conducted a thorough analysis of how the combination of EMG and EEG signals could be utilized in bio-robotics, emphasizing the primary benefits of this method. While EMG-EEG is recognized as a potential interface for robotic manipulators and end-effectors, its use in wearable arm exoskeletons remains limited. Kawase and his team created a real-time exoskeleton tailored for paralysis patients using both EMG and EEG, with EMG determining joint angles. Another study introduced an artificial neural network model optimized for instinctive control of an arm exoskeleton, where EMG predicted grabbing actions and EEG predicted arm movements.

The dual use of EMG and EEG provides distinct advantages for exoskeleton control by tapping into both muscle and cerebral activities. This dual-input system can offer predictions of motor actions and user intentions and also serves as a valuable tool for evaluating rehab treatments. However, capturing and synchronizing both EMG and EEG data demands a more sophisticated design and control approach.

2.2 Soft Exoskeleton Actuators

In Figure 2.12, we can see various soft exoskeleton arm robots with various types of actuators.

Figure 2.12

Upper Limb soft Exoskeletons and Types of Actuations



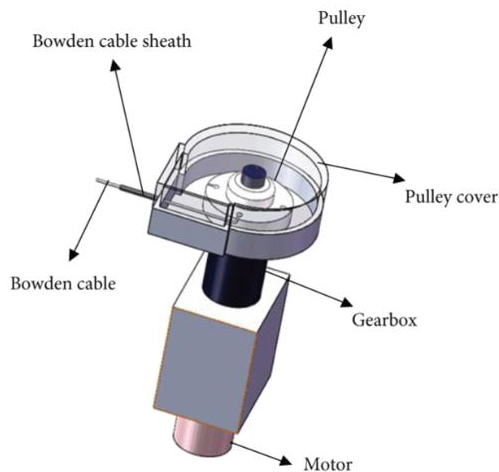
2.2.1 Cable Actuation

This type of actuations usually uses a Bowden cable as shown in figure 2.2.3. These are usually made of steel or nylon to create tension or compression forces where one end is connected to the input where the force takes place and the second is the output where the actuation takes place over some distance. Saiful. (2023). Wei et al. (2018) Introduced a design for a soft upper limb exoskeleton aimed at rehabilitation training, incorporating insights from human biomechanics. The innovative soft driving structure, utilizing Bowden cables, is devised to address potential joint damage and arm discomfort arising from man-machine interaction forces. Structural optimization is a key focus to minimize these interaction forces, and simulations in ADAMS involve adjusting the number and location of force-bearing points, particularly in the elbow movements. The study employs a human arm model for motion simulations and utilizes a mathematical model based on Bowden cable transmission to describe shoulder skeletal system movements. Experimental data analysis, aided by a man-machine contact force sensor, reveals that increasing the number of force-

bearing points and moving them away from the elbow effectively reduces man-machine interaction forces.

Figure 2.13

A 3d Model of the Bowden Actuation



Samper-Escudero et al. (2020) presented a textile-wearable soft exoskeleton designed to assist shoulder and elbow flexion. The cable-driven actuation is integrated into a jacket, utilizing various textiles and deformable components. Challenges associated with textile use, such as slipping, dampening, and pressure sores, are addressed through a combination of textile layers and force-compliant sewing. The design incorporates specialized elements for cable guidance, anchoring, and support, employing diverse tailoring techniques for simplified fabrication, wearability, and cleaning. Motors and electronics, designed to be textile-compatible, are housed in a backpack, reducing forces from dynamic loads and alleviating arm weight. The emphasis is on enhancing autonomy and assistance through the optimization of cable routing and friction reduction.

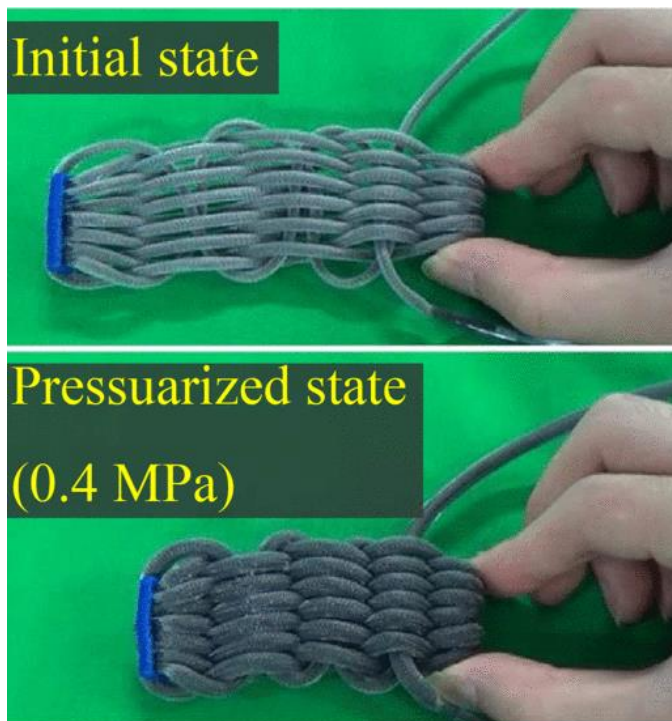
2.2.2 Pneumatic Actuators

Pneumatic actuator is basically converting the compressed air into mechanical motion. It is beneficiary for position control in a system. Whereas, hydraulics actuators uses fluid pressure to mechanical motion. It is necessary where high force is required. Abe et al. (2019) introduced a new winding technique for a pneumatic artificial muscle. Using this approach, the inflation of silicone tubes is converted into muscle contraction, with the expansion occurring on only one side of the muscle. This means that the actuator's expansion does not impact nearby objects.

Consequently, this muscle design is well-suited for wearable robots, ensuring there is no compression on the user's skin. The paper presents simplified models for the contraction ratio and force, which are validated through experiments. The prototype discussed in this paper achieves a maximum contraction ratio of 35.8% and a maximum output force of 12.24 N, all within a slim 5 mm thickness. Its high compatibility makes it an excellent alternative for wearable robots.

Figure 2.14

18 Weaves McKibben Muscle



2.3 Control

Control systems are a way that uses algorithms and rules to state the desirable behaviors of a system. It can be used to control the speed and precision of how the robot moves. Example, assembly robot, self-driving vehicles and even elevators. These control systems are backed by sensors that give feedback about the condition or states of the robot and then the actuators respond by the mathematical equation or rules set out by the engineer to behave in a certain desirable way.

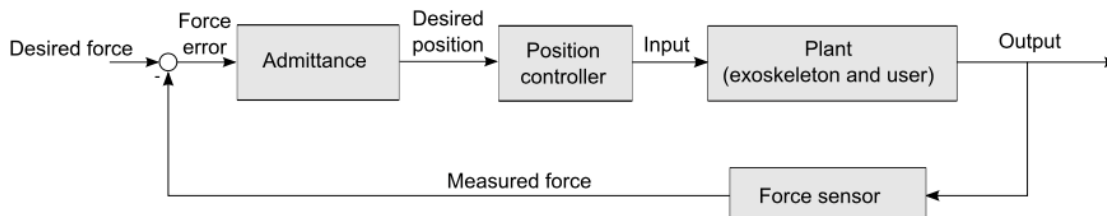
There is a wide domain to explore in control systems, but the project aims to use lower standard of control for the exoskeleton. As for closed loop control, we should only use those variables that we can control and measure.

2.3.1 Impedance and Admittance Control

Impedance and admittance control techniques are inspired by biological systems and revolve around the interchange between position and torque. The impedance controller's objective is to produce an interaction force based on the position error, like ensuring the task trajectory remains undisturbed. On the other hand, admittance control seeks to enable movement based on force/torque feedback, enhancing the interface between humans and exoskeletons. Within the realm of rehabilitative exoskeleton designs, these controllers can operate in either the task space or the joint space. Controllers working in the task space, also known as Cartesian space, are generally favored because they directly pertain to the design of task trajectories and task-space movements are three-dimensional, unlike the multi-dimensional joint space. The choice and positioning of sensors should be consistent with the chosen control approach. In essence, for all design scenarios, the combination of sensors, control mechanisms, and additional equipment should be integrated based on the specific tasks at hand.

Figure 2.15

Impedance and admittance control (EduExo,2023)



Da Silva et al. (2020) Presented a hybrid-controlled exoskeleton robot where impedance controllers are combined with biological signals to amplify human inputs and integrate adaptive mechanisms for flexible impedance control. One notable study presented a combined impedance-admittance control approach that utilized EMG data in real time for a 2DOF robot arm, the average error from shoulder and elbow was rendered to be 2.452% with no payload. The system could be better by having control variables with regard to the posture variations of the subject or patient.

Kim et al. (2014) presented presented force and impedance controller in their exoskeleton to compute the coupling torque to get the well-coordinated and natural movement of the shoulder, called SHR (Scapulohumeral Rythm The impedance controller then does this by obtaining the

reference angles of shoulder girdle with respect to the upper limb angle, using the reference angles of the shoulder girdle. Furthermore, they used Newton-Euler recursive algorithm to achieve it. The device performed well on the experiments conducted to render kinematics and dynamics to exhibit the task-space force and impedance control as desirable outcome.

Figure 2.16

2 DOF Exoskeleton with Impedance Control



2.3.2 Adaptive Control

Adaptive control systems can automatically adjust to changes in dynamic models with fluctuating parameters, ensuring that any inconsistencies in system dynamics are addressed. In contrast, SMC (Sliding mode control) control is dependent on time. By merging SMC and adaptive control, adaptive SMC has been realized. Kang et al. (2013) created a strategy to support the safety of a five-DOF upper limb exoskeleton. Their adaptive control design focused on precise trajectory following, enhanced resilience to faults, and safety. The refinement of exoskeleton design is pivotal for upper limb exoskeletons. Nasiri et al. (2021) introduced a novel adaptive control system for fine-tuning assistance levels in exoskeletons, leveraging a blend of adaptive feedforward and feedback controls. Brahmi et al. (2018) put forth an adaptive control method for tracking that utilized a backstepping procedure paired with time-delay estimation to ascertain unanticipated dynamics and offset any external disturbances within set limits. Alshahrani et al. (2021) showcased a four-DOF upper limb exoskeleton that employed both synchronous ipsilateral control and a mirror control system transitioning from ipsilateral to contralateral, granting intentional control over the exoskeleton for the upper limb.

Figure 2.17*Control Techniques with Non-Bio Sensor Feedback*

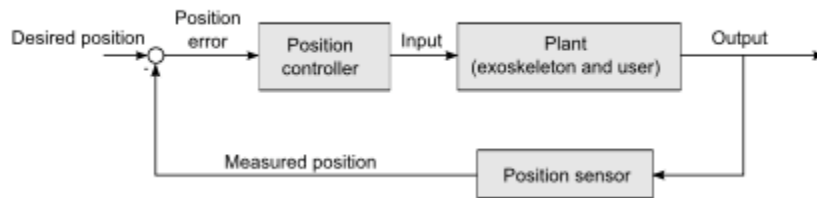
Control method	Control mode	Support provided	Coordinate system evaluation	Sensor type
PID-sliding mode	Adaptive control		Modified DH parameters	
Adaptive control	Adaptive control		DH parameters	
MCS	Adaptive impedance control	Active	DH parameters	Force, load sensor
SMC, JSTDE	Adaptive control			Hall sensor, force sensor
SMC	Adaptive control	Active	Modified DH parameters	Hall sensor, force sensor
SMC, CTC	Adaptive control	Simulated		
FSR	Admittance control	Active	Jacobian matrix	Force sensor
SMC		Simulated	Jacobian matrix	Force sensor
FSMC		Simulated	DH parameters	
MCS, load cells	Adaptive impedance control		Jacobian matrix	
SMC	Adaptive control	Passive	Jacobian matrix	Force, torque
SMC	Adaptive control	Passive		
SMC	Adaptive control	Passive	Jacobian matrix	
MCS	Adaptive control	Active/Passive	Jacobian matrix	Force, load

2.3.3 Position Control

The position controller is used for controlling a specific position like joint angles of a linked manipulator robot. Furthermore, it aids in moving the links in a desired output angle. The torque value varies until it reaches the desired outcome.

Figure 2.18

Position Control Block Diagram



Crea et al. (2017) presented an arm exoskeleton robot for the rehabilitation of elbow movement with position control and torque control. In the case for position control, the links or joints move in desired angle output trajectory in a closed loop. They used proportional Integrative regulator which determines the error for desired to measure joint.

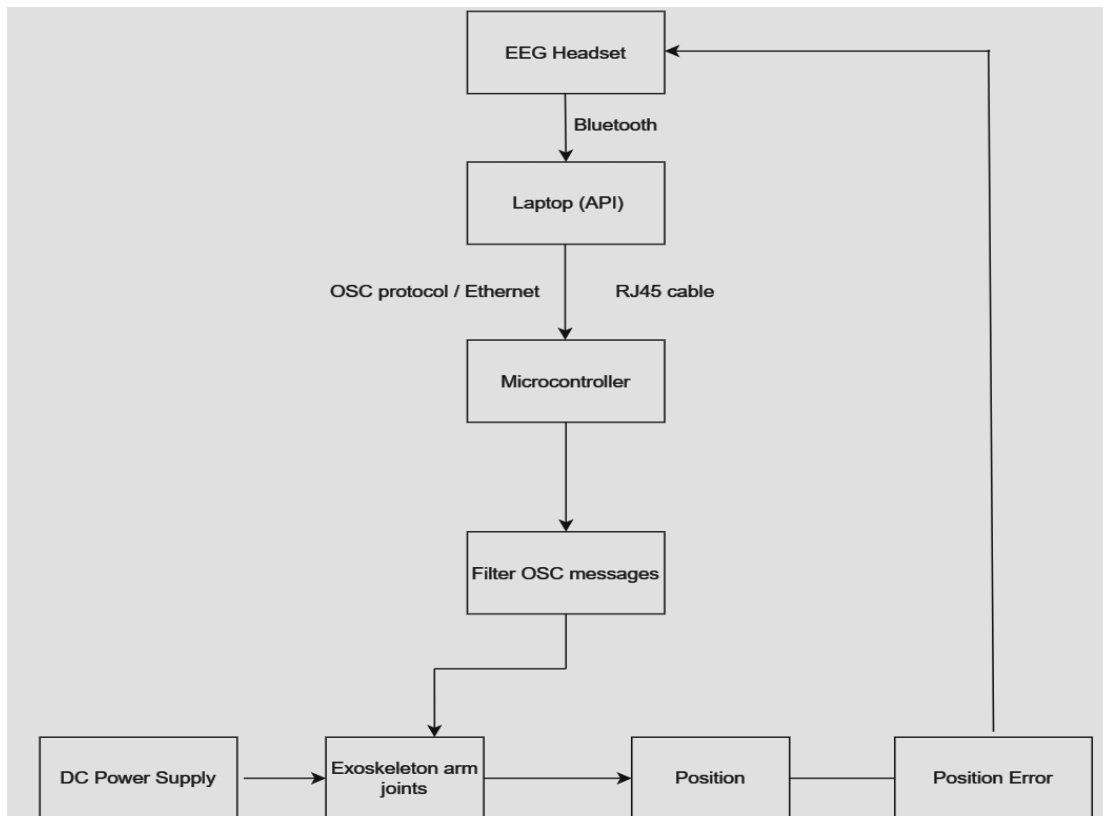
CHAPTER 3 METHODOLOGY

3.1 Overview of System

From the Figure in 3.1, The exoskeleton arm robot receives commands from the EEG headset, Emotiv insight 2 via the main micro controller which filters the OSC messages of motor movements to execute the positive and negative movements of the two joints of the robot. A combination of these commands from the user of the EEG headset moves the joint to pick an object from the gripper as the end effector from one point and tries to control the degree of the joints to place the object to another point / box.

Figure 3.1

System Overview Block

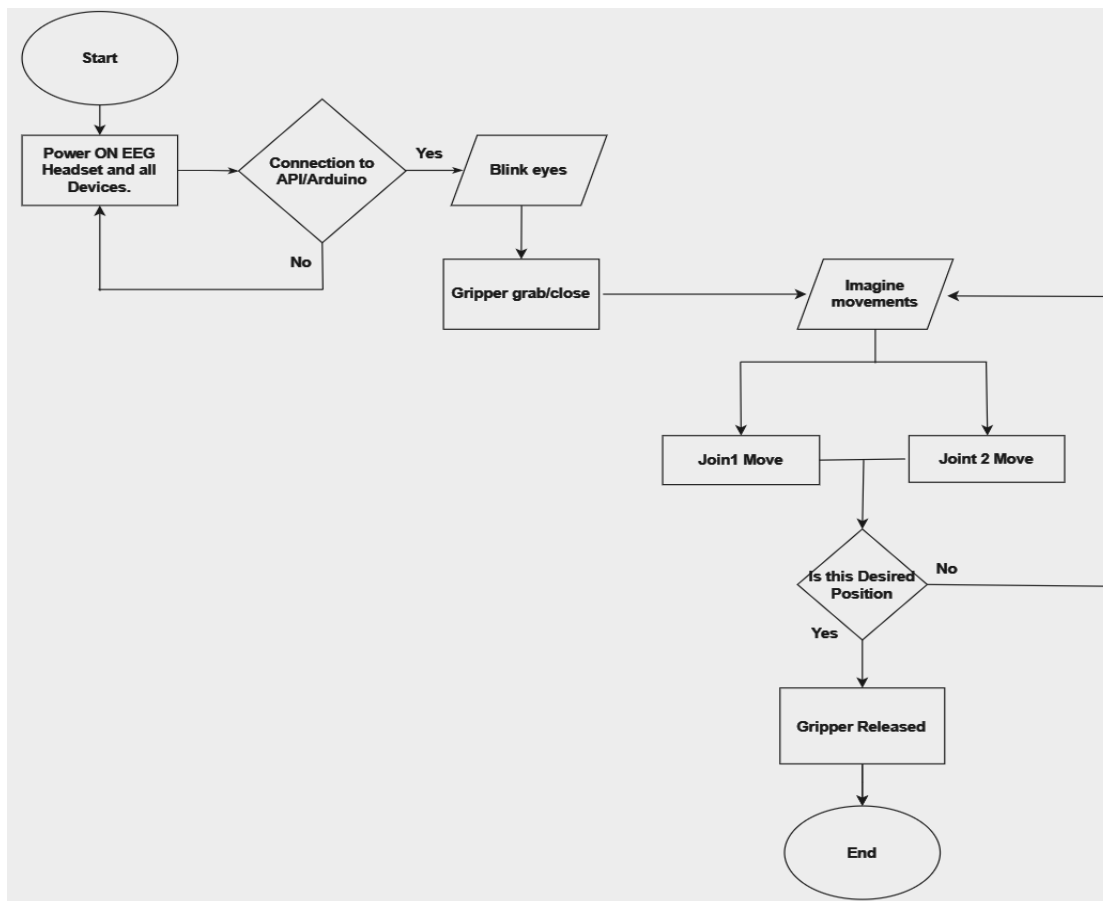


The Arm exoskeleton robot is placed in an initial position with the gripper ready to pick and object. The EEG headset, Emotiv Insight is connected to the host PC via Bluetooth. The Emotiv's api then

requests for the user's trained mental commands namely, neutral, push, pull and lift. These mental commands are streamed through OSC(Open sound) protocol via ethernet cable from host computer to Arduino mega via Ethernet shield. The Arduino first maintains connection to receive the OSC messages, buffers the commands from 0 to 10 range for each mental commands like neutral, push, pull and lift. Then, the intensity of the OSC command for each command is mapped to match the servo's movement to give a sense of control to user for controlling the degree of movement of the joints instead of the servo moving in absolute angles.

Figure 3.2

Flowchart of the Working of the System



3.1.1 System Controllers

There are two types of controllers in the system. One is the EEG headset that plays the most important part in the system to send rapid OSC messages from the user's imagination and the other is the Arduino that filters these extremely varying OSC messages and buffers them, so that a combination of joint movements can achieve pick and place. The user trains and saves data, so that the next time user uses the EEG head, it can match the movements imaginations they trained on. These commands are sent via OSC protocol in floating values. Hence, an ethernet is used to connect the pc and Arduino to have the OSC protocol sent locally which is useful when you want instant real time / delay less communication.

The EEG headset is a device designed for research of brain waves and brain machine interface applications. It has five channels plus two reference sensors, capturing brain activity across key areas. The high-resolution data acquisition allows users to monitor brainwaves and translate them into meaningful metrics and use that to control robots or computer applications. The Insight 2 is wireless, making it both portable and versatile and testing and prototyping is much easier.

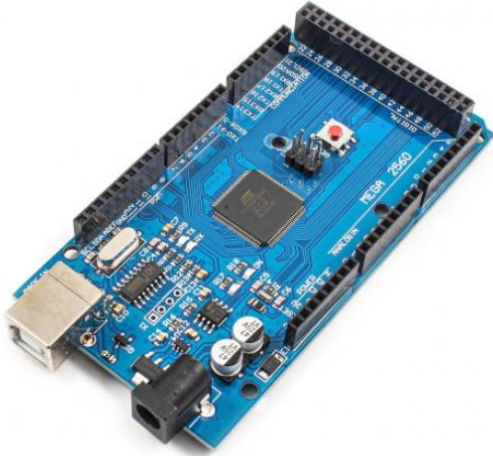
Figure 3.3

Emotiv Insight 2 Headset



Figure 3.4

Arduino Mega Micro-Controller



The Arduino Mega 2560 is built around the ATmega2560 microcontroller, featuring 54 digital input/output pins, including 15 pins for PWM outputs, and 16 analog inputs. It is equipped with 4 UARTs for hardware serial communications, a 16 MHz crystal oscillator for timing, a USB port for programming and communication, a power jack for external power supply, an ICSP (In-Circuit Serial Programming) header for bootloader programming, and a reset button for restarting the board.

As discussed in previous section, the Arduino microcontroller filters the osc messages and tries to allow the correct commands to make the pick and place work. Furthermore, it also maps the intensity of the OSC messages from the EEG headset to make the joints move accordingly to give a sense of control in the degree of movement.

3.2 Mechanical Design

The design is made with 3d printed filaments, load sensor, amplifier and high torque servos. The design of the exoskeleton is inspired by an open source 3d model from EduExo (Volker Bartenbach, 2017).

Figure 3.5

Design of Karuna Robot

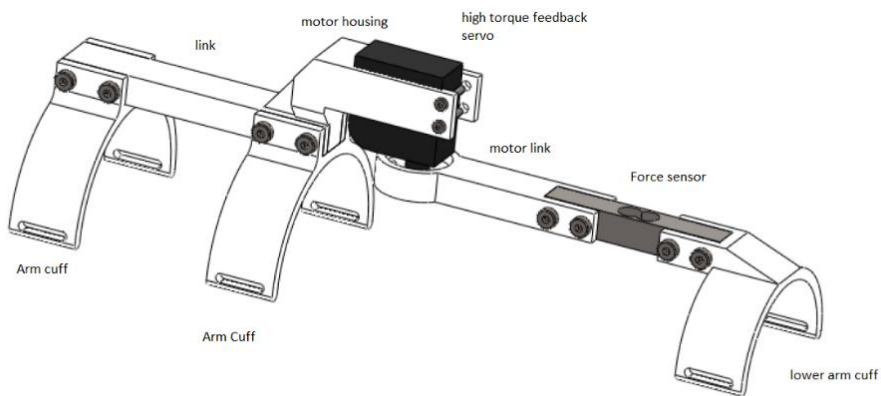


Figure 3.6

Motor Housing

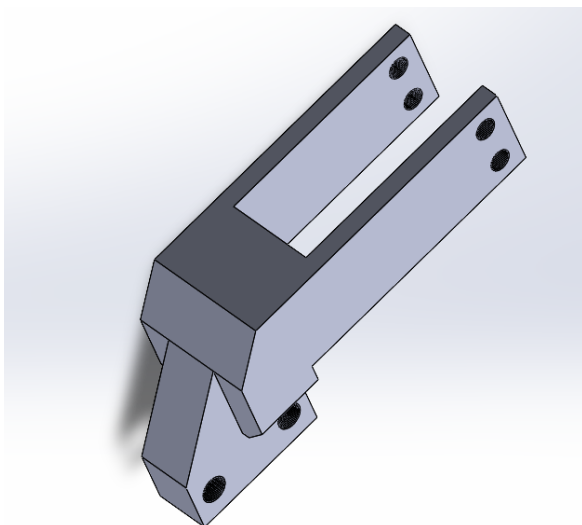


Figure 3.7

Motor Interface

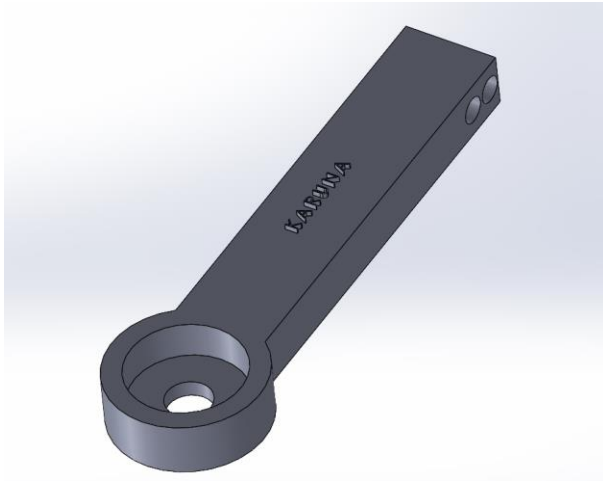


Figure 3.8

Link

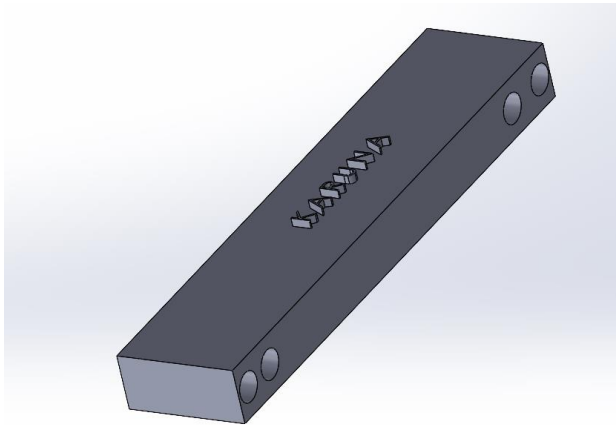


Figure 3.9

Cuffs (2)

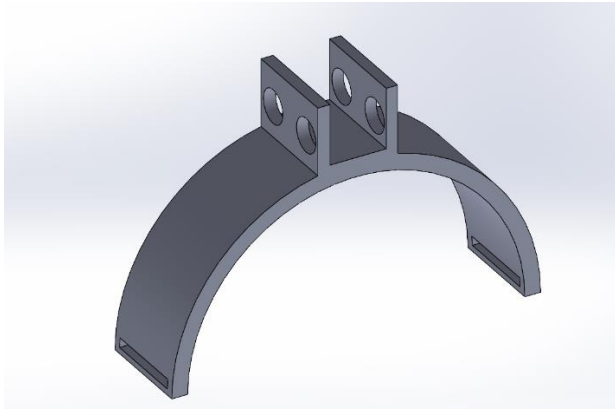


Figure 3.10

Motor Housing



Figure 3.11

Gripper (Open-source Gripper on Grabcad website (Anand, 2023))



3.3 Data Structure: Circular Queue and Linear Interpolation

In order to have a sequenced and desirable result of performing joint movements, tracking them as well as performing pick and place, A circular Queue method is used to buffer and manage the OSC messages from the headset and API that could result in random and undesirable movements. We specifically want mental commands like neutral, push, pull and lift to be queued.

It is a circular linear data structure and follows the first in and first out. Unlike linear circular data structure, where after the addition of last element, we cannot add another element even if there are empty spaces before the front element. To combat this, after the queue is full in the last position, new elements can be added again from the first position. Then, use dequeue to remove the elements and add new elements to save space and can run the neutral, push, pull and lift.

Moreover, the use of Linear interpolation to map the OSC messages which range from 0 – 10 with servo movements to use floating values to resonate and mimic our desired degree of movement.

The equation is as follows:

$$y = y_1 + (y_2 - y_1) / (x_2 - x_1) \times (x - x_1)$$

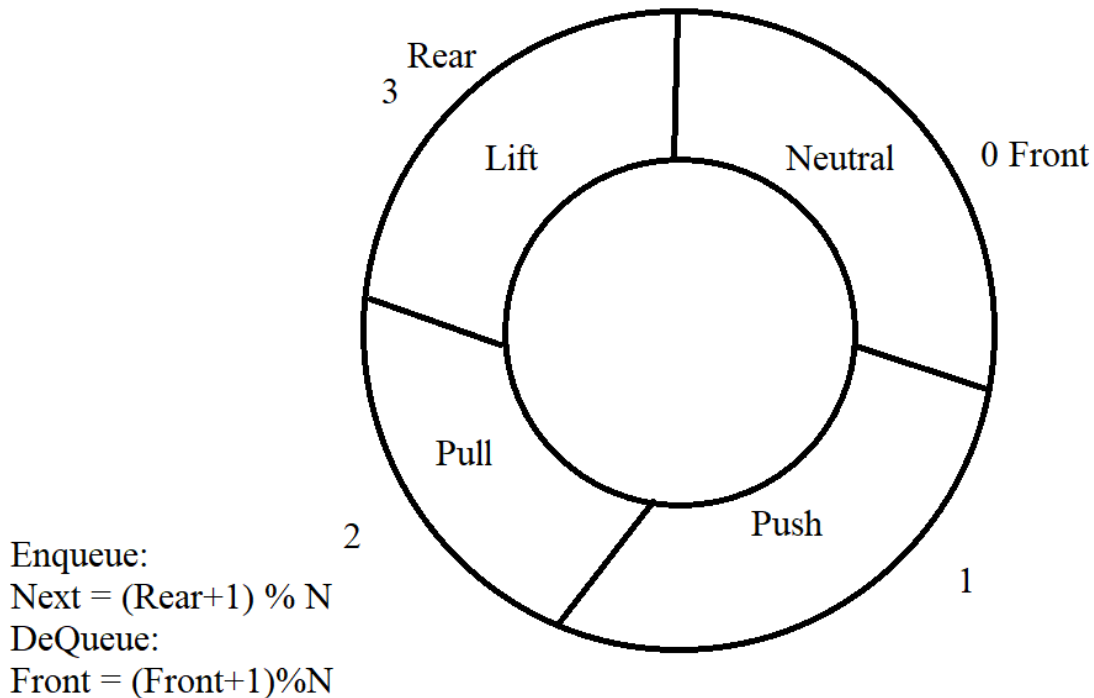
Here,

X and Y values are unknown and are the OSC messages from the EEG headsets that can be push, pull, lift or neutral mental commands. Then, Y1, Y2, X1 and X2 are the lower and upper ranges

or initial position and target position in the servo and the lower and upper range of OSC message, 0-10. Thus, by using this logic, we map the intensity of the mental commands and use it to control the degree of movement of Karuna Robot.

Figure 3.12

Enqueue Method for Mental Commands.



In figure 3.12, we have a circular queue where the front and rear node begin from 0 position from -1. Then, we set both front and rear in 0 position then perform enqueue on rear node to have Neutral at 0. Then, rear node is set to 1 after $(Rear+1) \% N$. This way we can populate the arrays until we have enqueued our four commands Neutral, push, pull and lift. Then, we can begin dequeue by performing $Front = (Front + 1) \% N$ which will bring the position of front node to 1 from 0, then 1, 2 and 3. In the meantime, enqueueing also takes place rapidly so we always have the sequence we want. The time complexity for enqueue is $O(1)$ which makes it ideal for faster execution of tasks.

Figure 3.13

Complete Mechanical Design of Karuna Robot



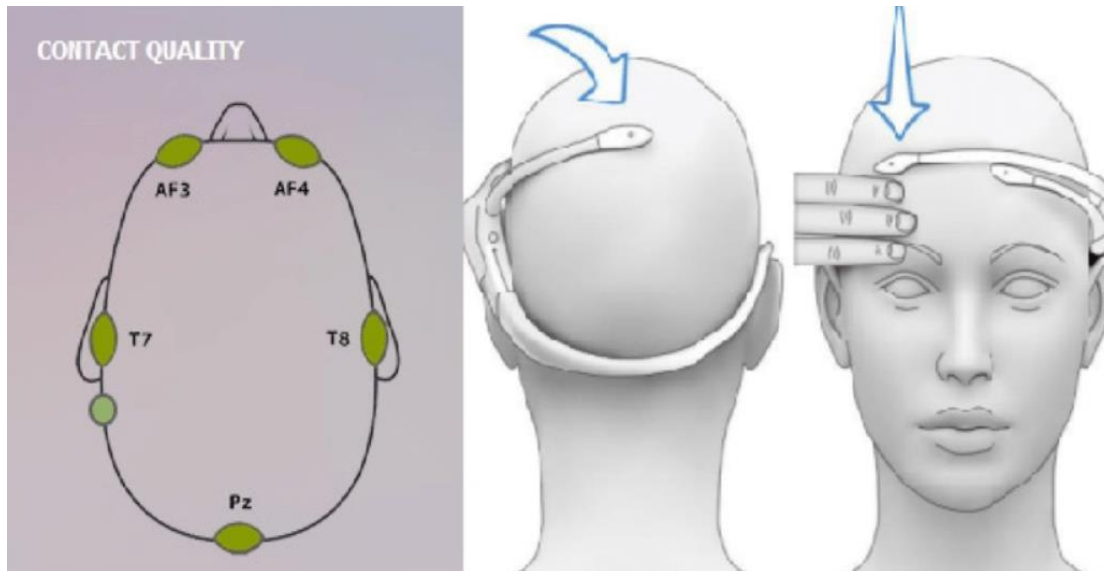
The final design for Karuna robot involves a 2 DOF exoskeleton robot with a gripper as end effector and 3.4Nm servos. It is mounted on aluminum profiles to provide support and space to perform pick and place.

3.4 Brain Machine Interface System

The 5 Channel EEG headset, Emotiv insight 2 renders the brain activities and signals.

Figure 3.14

5 Channel EEG Headset: Emotiv Insight 2 (Hendradi, 2018)



The headset used is a 5 channel namely, AF3, Af4, T7, T8 and Pz headset Emotiv Insight 2.0, with 0.5-43Hz and with digital notch filter from 50 to 60 Hz. Furthermore, it has sampling rate of 128 SPS. (Emotiv, 2024). Each of these 5 electrodes correspond to specific parts in the brain and each has specific readings for the same. The three parts of the brain that these electrodes give readings are from the frontal lobes which are useful for motor moment planning and reasoning. Whereas, Temporal lobes are responsible for the recalling of the memories related to motor and auditory. As for Parietel, it is known for being able to distinguish between senses felt from all over the body regarding touch, temperature etc. (Lobes of the Brain, 2016).

Table 3.1*EEG Electrodes and their Meaning*

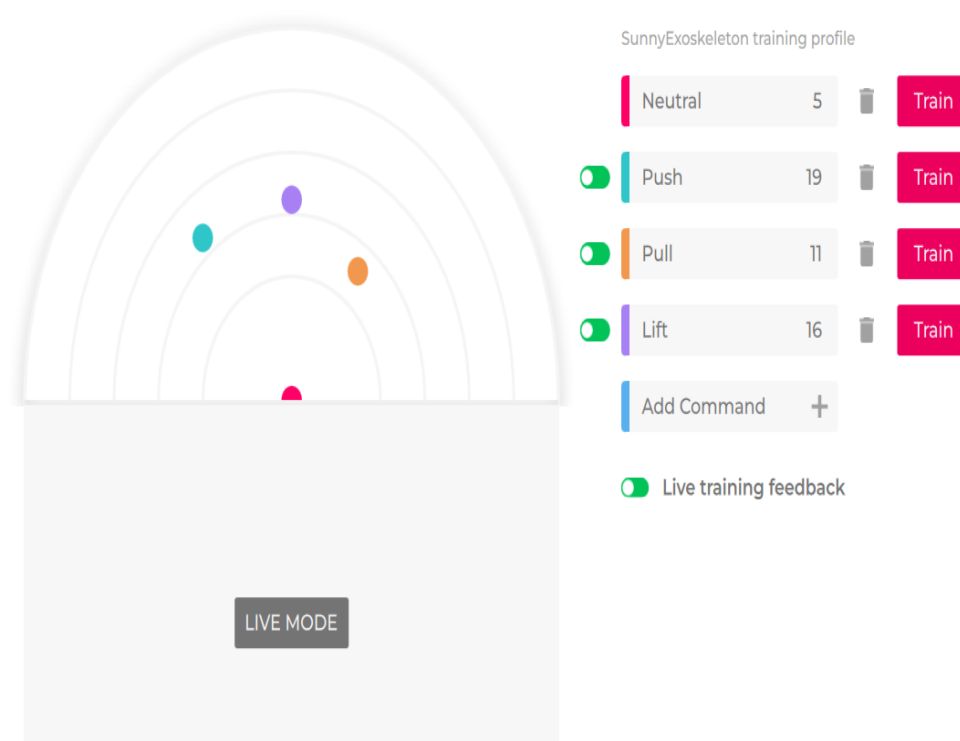
Lobes	Electrodes	Function
Frontal	AF4, AF3	Motor Planning
Temporal	T7, T8	Memory, Audio
Parietal	Pz	Sensations, attention

3.4.1 Experimental Setup

The User is given enough time to train each specific mental commands by making simple and repeatable movement imagination in their head and train in the Emotiv's Desktop Application. The user gets feedback on the accuracy of successfully performing the imagination of movement by interpreting the box movement corresponding to their imagination.

Figure 3.15

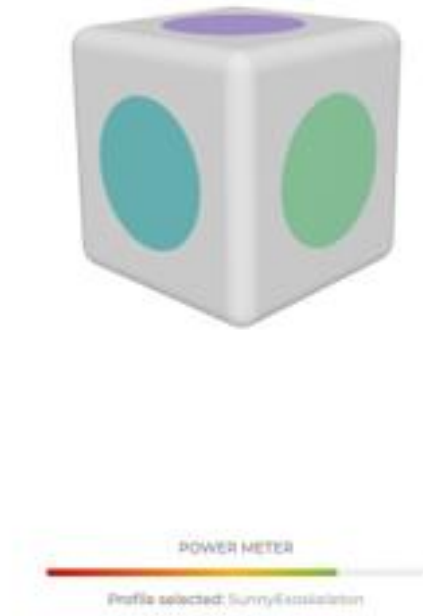
Training Mental Commands



The Figure 3.15 depicts user's personal training profile. The more the user trains the mental commands, the more accurate the prediction of mental command is.

Figure 3.16

Feedbacks Box for Mental Commands

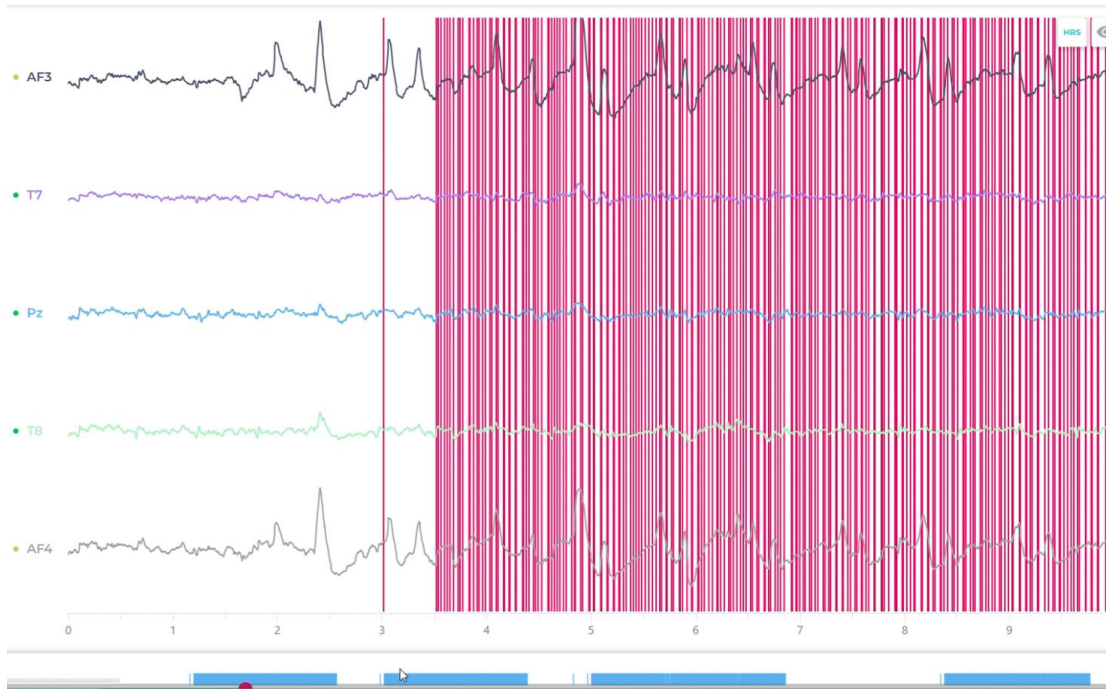


3.4.2 Signal Collection and Pre-Processing

The signal collection is done via Emotiv Insight 2 device in Figure 3.3 above. 5 electrodes are placed in the head to retrieve information from AF4, AF3, T7 and T8 at 128 Hz sampling frequency. The raw EEG data is recorded offline via the Emotiv pro application provided by the company. The raw EEG data was recorded and saved as a .csv file. The recording involved a baseline recording in the beginning with two activities of closing and opening eyes for 15 seconds each. Then, manual keystroke time marking was done to allow around 20 seconds each for the user to think of each mental commands.

Figure 3.17

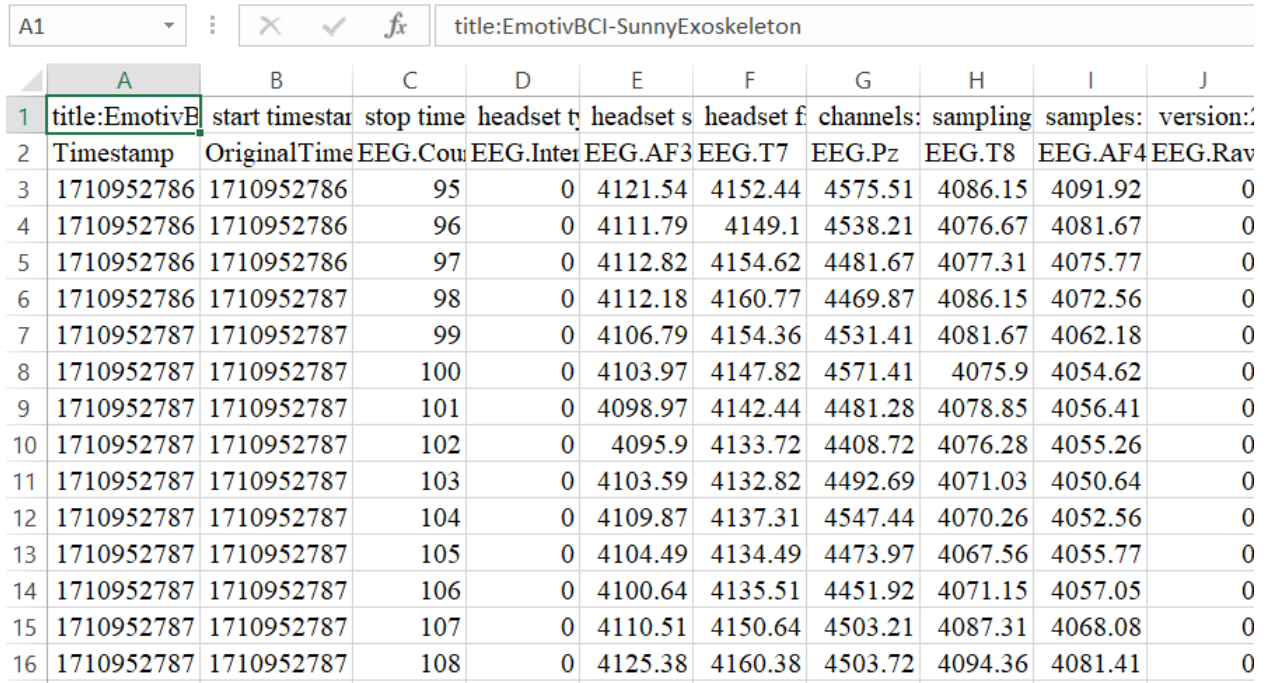
Raw EEG Data Recording



In figure 3.17, we can see the raw EEG recordings across all the electrodes: AF3, T7, Pz, T8 and AF4. We can also see red vertical lines above which were keystroke generated in order to get the window to analyze each mental state for 20 seconds each.

Figure 3.18

Raw EEG Data to .CSV Files in Time Series



	A	B	C	D	E	F	G	H	I	J
1	title:EmotivB	start timestar	stop time	headset t	headset s	headset f	channels:	sampling	samples:	version:..
2	Timestamp	OriginalTime	EEG.Cou	EEG.Inter	EEG.AF3	EEG.T7	EEG.Pz	EEG.T8	EEG.AF4	EEG.Rav
3	1710952786	1710952786	95	0	4121.54	4152.44	4575.51	4086.15	4091.92	0
4	1710952786	1710952786	96	0	4111.79	4149.1	4538.21	4076.67	4081.67	0
5	1710952786	1710952786	97	0	4112.82	4154.62	4481.67	4077.31	4075.77	0
6	1710952786	1710952787	98	0	4112.18	4160.77	4469.87	4086.15	4072.56	0
7	1710952787	1710952787	99	0	4106.79	4154.36	4531.41	4081.67	4062.18	0
8	1710952787	1710952787	100	0	4103.97	4147.82	4571.41	4075.9	4054.62	0
9	1710952787	1710952787	101	0	4098.97	4142.44	4481.28	4078.85	4056.41	0
10	1710952787	1710952787	102	0	4095.9	4133.72	4408.72	4076.28	4055.26	0
11	1710952787	1710952787	103	0	4103.59	4132.82	4492.69	4071.03	4050.64	0
12	1710952787	1710952787	104	0	4109.87	4137.31	4547.44	4070.26	4052.56	0
13	1710952787	1710952787	105	0	4104.49	4134.49	4473.97	4067.56	4055.77	0
14	1710952787	1710952787	106	0	4100.64	4135.51	4451.92	4071.15	4057.05	0
15	1710952787	1710952787	107	0	4110.51	4150.64	4503.21	4087.31	4068.08	0
16	1710952787	1710952787	108	0	4125.38	4160.38	4503.72	4094.36	4081.41	0

We acquire the csv file from the Raw EEG data in time series as show in Figure 3.18. This is an unprocessed EEG data and may not be able to provide meaningful data. Thus, we need to perform preprocessing and Fast Fourier transform to the above to get EEG data in frequency domain. A high band pass filter of second order is applied at 0.5Hz to reduce noise and the slew value is limited to 30mv. Then, Waves such as Theta (4-8Hz), Alpha (8-12Hz), Low beta. Moreover, The Fourier transform window length used was 256 and the sliding window step size was 64.

Once the EEG is preprocessed and change to frequency domain, it renders another csv file like in Figure 3.19.

Figure 3.19

Preprocessed EEG Data in Frequency Domain

	A	B	C	D	E	F	G	H	I	J	K	L	M	N
1	stamp_i_desc	stamp_f_desc	latency_i	latency_f	minimum	maximum	data_fixe	eeg.af3_4	eeg.t7_4	eeg.pz_4	eeg.t8_4	eeg.af4_4	eeg.af3_8	eeg.t7_8
2	1700093905	1700093907	0	1.99152	4	56.3314	0	6.66367	0.03112	9.16059	-0.0341	7.72629	3.80237	-3.7431
3	1700093905	1700093907	0.49983	2.49135	4	35.5832	0	3.34797	4.69304	1.71151	-0.5852	3.94866	0.95899	0.48436
4	1700093906	1700093908	0.99966	2.99118	4	34.1732	0	2.78855	6.65604	3.37469	0.02751	3.01872	-1.6202	2.3593
5	1700093906	1700093908	1.4995	3.49101	4	34.2136	0	3.03167	3.79318	9.16	2.99805	2.47939	-0.5326	-0.1608
6	1700093907	1700093909	1.99933	3.99085	4	48.2584	0	9.61636	11.0731	10.2409	9.71087	8.1962	4.10595	3.24583
7	1700093907	1700093909	2.49916	4.49068	4	53.0794	0	10.4921	12.2245	6.64983	10.5883	9.22932	4.72729	4.35832
8	1700093908	1700093910	2.99899	4.99051	4	55.0585	0	5.95153	8.75341	3.56448	4.64563	4.30248	2.61235	4.90058
9	1700093908	1700093910	3.49883	5.49034	4	46.2872	0	5.77417	10.1063	4.34293	4.39405	2.98511	1.4646	5.81545
10	1700093909	1700093911	3.99866	5.99018	4	27.745	0	1.63433	8.65774	3.20069	3.28629	2.07372	-0.4751	2.92593
11	1700093909	1700093911	4.49849	6.49001	4	27.8562	0	1.97264	4.35182	2.21967	2.70193	3.93939	-0.1744	1.87847
12	1700093910	1700093912	4.99832	6.98984	4	35.9568	0	3.71296	0.90577	6.26682	1.51685	4.33192	2.71492	0.79111
13	1700093910	1700093912	5.49815	7.48967	4	43.0906	0	6.55726	1.99715	7.50462	4.65351	7.13626	0.56039	-5.305
14	1700093911	1700093913	5.99799	7.98951	4	43.1288	0	5.30014	2.76511	5.68221	5.21347	5.38142	0.49519	-2.6557
15	1700093911	1700093913	6.49782	8.48934	4	40.4884	0	-0.5764	2.18892	5.68525	3.52283	1.2715	-0.579	-2.1073
16	1700093912	1700093914	6.99765	8.98917	4	29.225	0	2.0865	1.23395	3.61473	4.31076	4.30598	-0.1956	1.89962
17	1700093912	1700093914	7.49748	9.489	4	23.5603	0	5.43447	4.16204	8.96099	2.42664	6.21399	2.41901	5.68264
18	1700093913	1700093915	7.99732	9.98884	4	23.369	0	3.40404	0.8577	7.77029	4.51941	7.65274	2.16791	2.12352
19	1700093913	1700093915	8.49715	10.4887	4	24.3734	0	3.09664	0.80056	2.5897	6.92851	5.89052	1.66818	-0.9976
20	1700093914	1700093916	8.99698	10.9885	4	24.309	0	6.46027	4.39424	4.67595	4.54146	8.05288	1.75217	0.50854
21	1700093914	1700093916	9.49681	11.4883	4	23.666	0	3.65778	4.34113	12.1447	4.65492	4.06507	-1.2678	-1.2104

Then, by performing some manual tracking for band power during specific mental states like Neutral, push, pull and lift from the “stamp_i_desc” column and “stamp_f_desc” column in Figure 3.19, which is the starting point and final points. We can evaluate the average band power of all waves across electrodes during a specific mental state based on csv file in figure where events are marked during the EEG recording.

Figure 3.20*Mental Commands Trigger Time Stamps*

1	latency	duration	type	marker_v	key	timestamp	marker_id
2	4.06898	15.0107	Eyes_Ope	1	-1	1712133779	1
3	24.0937	15.0107	Eyes_Clo	3	-1	1712133799	2
4	48.1249	18.7751	Neutral	1	1	1712133823	3
5	48.6247	18.7751	Neutral	1	1	1712133824	4
6	48.6481	18.7751	Neutral	1	1	1712133824	5
7	48.6716	18.7751	Neutral	1	1	1712133824	6
131	90.1892	18.822	push	2	2	1712133865	330
132	90.2517	18.822	push	2	2	1712133865	331
133	90.2595	18.822	push	2	2	1712133865	332
888	123.132	27.1474	pull	3	3	1712133898	1087
889	123.139	27.1474	pull	3	3	1712133898	1088
941	145.132	19.1187	lift	4	4	1712133920	1240
942	145.163	19.1187	lift	4	4	1712133920	1241
943	145.218	19.1187	lift	4	4	1712133920	1242
944	145.226	19.1187	lift	4	4	1712133920	1243
945	145.265	19.1187	lift	4	4	1712133920	1244
946	145.296	19.1187	lift	4	4	1712133920	1245
947	145.312	19.1187	lift	4	4	1712133921	1246
948	145.351	19.1187	lift	4	4	1712133921	1247

In Figure 3.20, we can see the Neutral, Push, Pull and Lift Timestamps which helps in tracking down data from EEG to filter and evaluate the EEG data during these periods of time.

CHAPTER 4

RESULTS

4.1 Control Degree of Movement

A circular enqueue and dequeue method along with linear interpolation was used to match have sequential and nuance control of joints to move as per the intensity of the user's brain signals instead of having absolute positive or negative.

Moreover, in Table 4.1, we record all the final angles the joint 1 reaches with target angle being 30 degrees from its initial, 90 degrees for 20 trials. Then, we take Mean Absolute error and Root mean Square Error to analyze the error.

Mean absolute error is given by,

Figure 4.1

MAE and RMSE Formula (Acharya, 2021)

$$\text{RMSE} = \sqrt{\frac{\sum (y_i - y_p)^2}{n}}$$

$$\text{MAE} = \frac{|(y_i - y_p)|}{n}$$

y_i = actual value

y_p = predicted value

n = number of observations/rows

Table 4.1*Joint 1: 30 Degrees Movement from 90*

Trials	Final Angles	Initial Position	Target Angles
1	87	90	30
2	82	90	30
3	85	90	30
4	77	90	30
5	72	90	30
6	50	90	30
7	44	90	30
8	41	90	30
9	36	90	30
10	32	90	30
11	30	90	30
12	30	90	30
13	30	90	30
14	30	90	30
15	30	90	30
16	31	90	30
17	29	90	30
18	30	90	30
19	30	90	30
20	30	90	30
MAE	15.4 Degrees		
RMSE	26.18 Degrees		

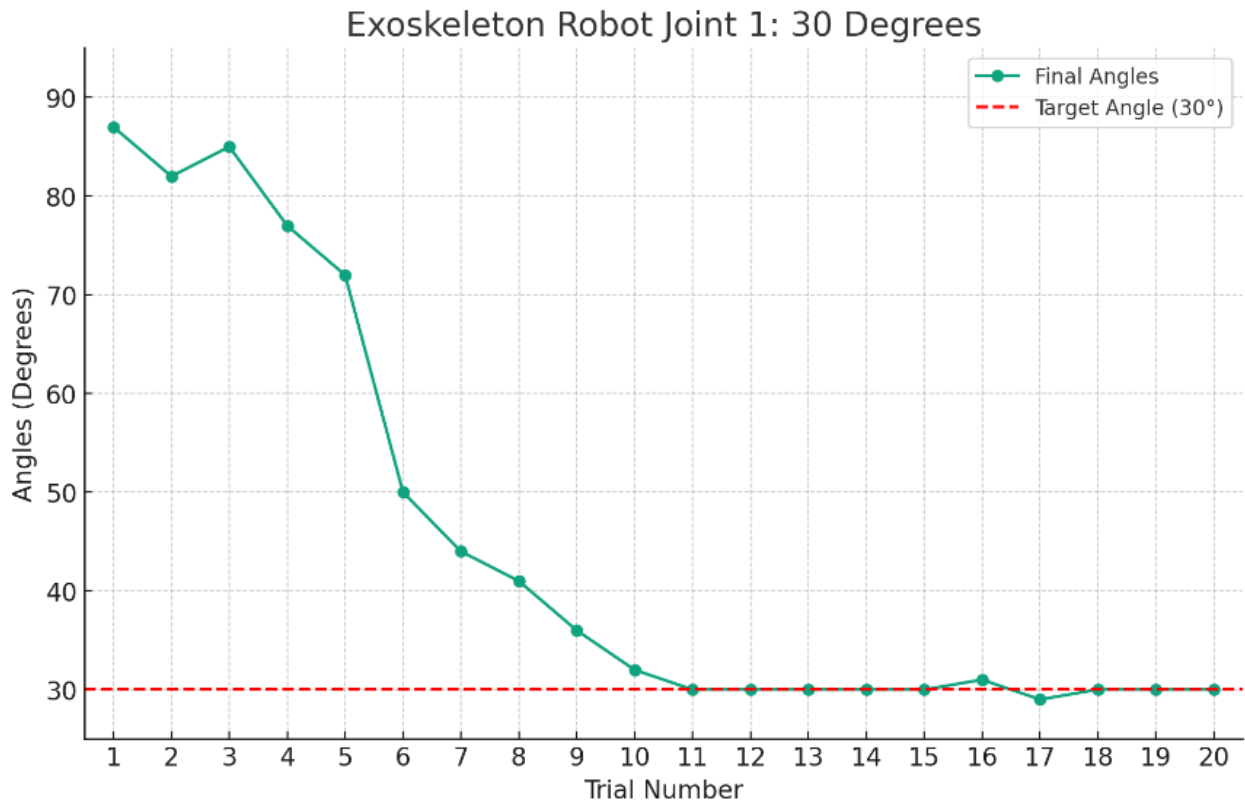
Figure 4.2

Exoskeleton Robot Joint 1: 30 Degrees from 90



Figure 4.3

Joint 1: 30 Degrees from 90 graph



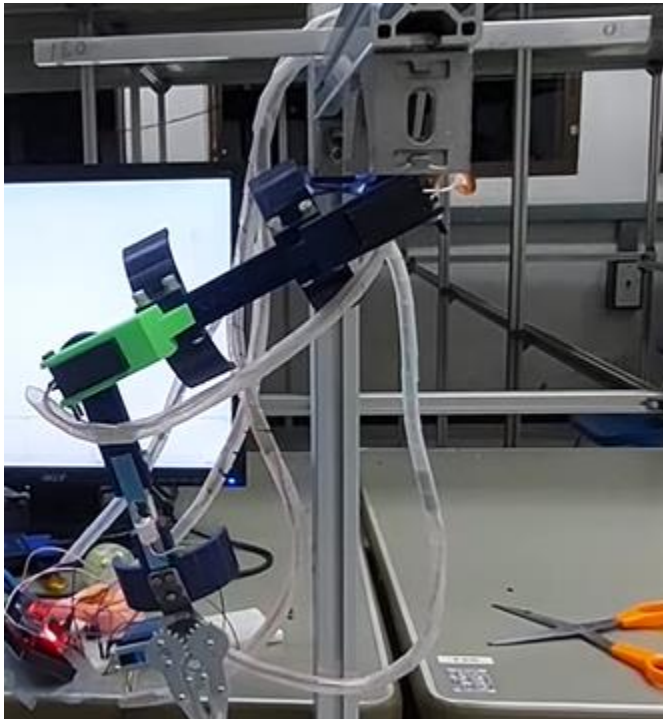
The servo maps the intensity of signal it receives from the EEG to mimic the movement of user's intention to move joint 1 to 30 degrees. We can evaluate from the Mean Absolute Error, 15.4 degrees and the Root Mean Square Error, 26.18 degrees, that there are some big deviations in the initial trials which is contributing in the significant average errors.

Table 4.2*Joint 1:180 Degree Movement from 90*

Trials	Final Angles	Initial Position	Target
1	111	90	180
2	127	90	180
3	133	90	180
4	164	90	180
5	164	90	180
6	164	90	180
7	164	90	180
8	164	90	180
9	171	90	180
10	171	90	180
11	171	90	180
12	171	90	180
13	171	90	180
14	172	90	180
15	172	90	180
16	172	90	180
17	173	90	180
18	173	90	180
19	173	90	180
20	173	90	180
MAE	17.3		
RMSE	24.34		

Figure 4.4

Joint 1 Attempt to Move to 180 Degrees



In Figure 4.4, we can assess from MAE, 17.3 and RMSE, 24.34 that we have significant errors in joint 1 reaching 180 degrees. From the table 4.2, We can assess that the join is not able to fully reach 180 degrees, this is because of mechanical obstruction as joint one has to deal with more load against the gravity.

Figure 4.5

Joint 1 180 Degrees Graph

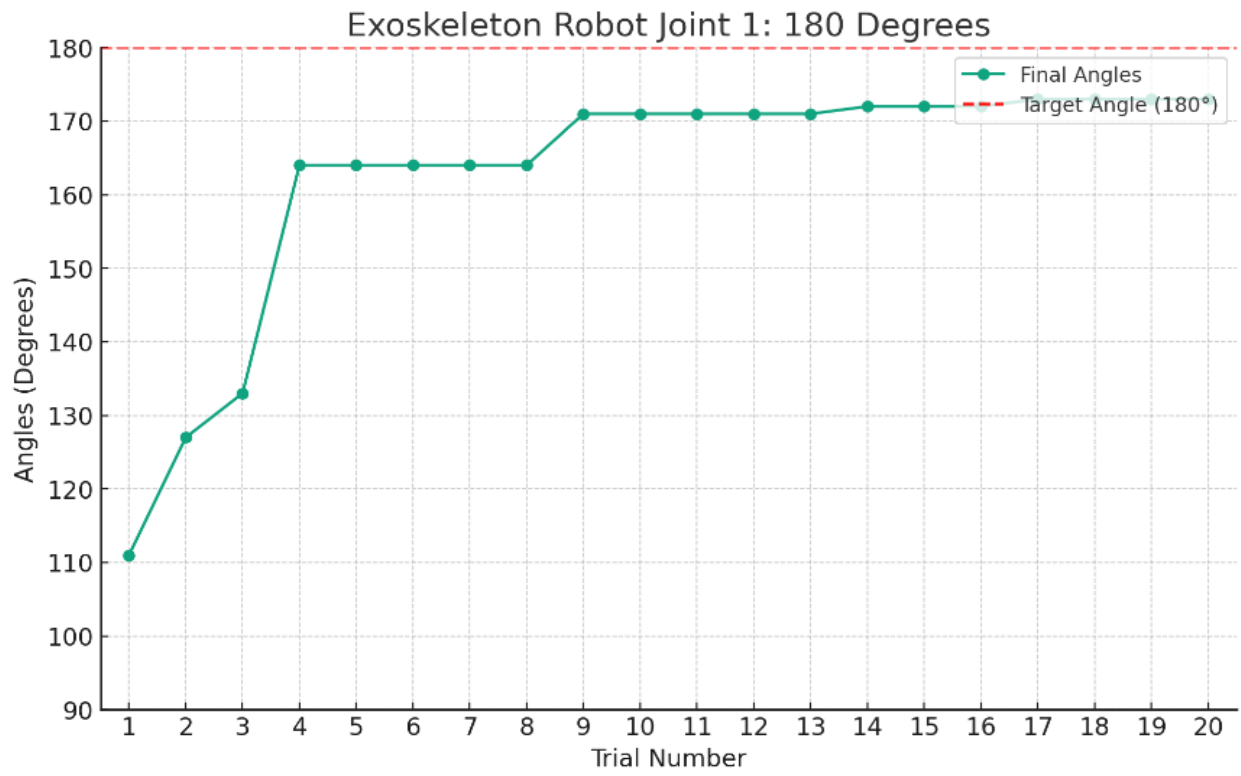


Table 4.3*Joint 2: 45 Degree Movement from 90*

Trials	Final Angles	Initial Position	Target Angle
1	43	90	45
2	45	90	45
3	46	90	45
4	47	90	45
5	44	90	45
6	41	90	45
7	44	90	45
8	45	90	45
9	46	90	45
10	43	90	45
11	44	90	45
12	43	90	45
13	44	90	45
14	43	90	45
15	45	90	45
16	44	90	45
17	43	90	45
18	44	90	45
19	43	90	45
20	45	90	45
MAE	1.3		
RMSE	1.61		

Figure 4.6

Joint 2 45 Degrees Movement

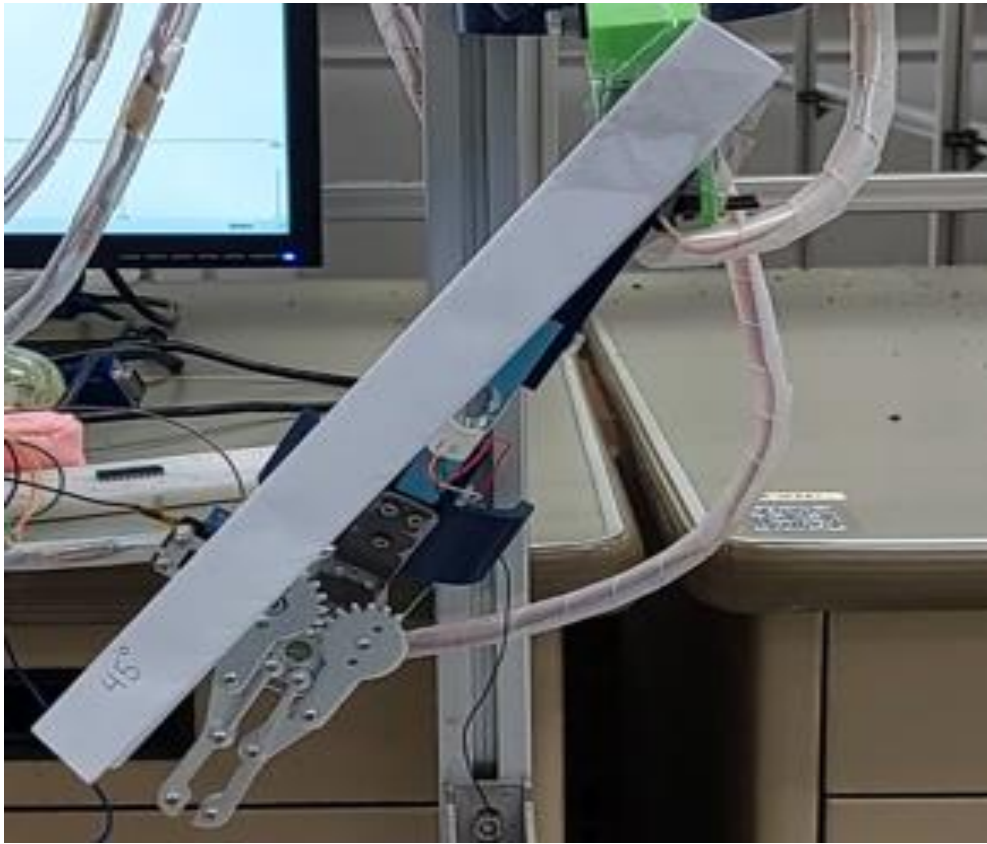
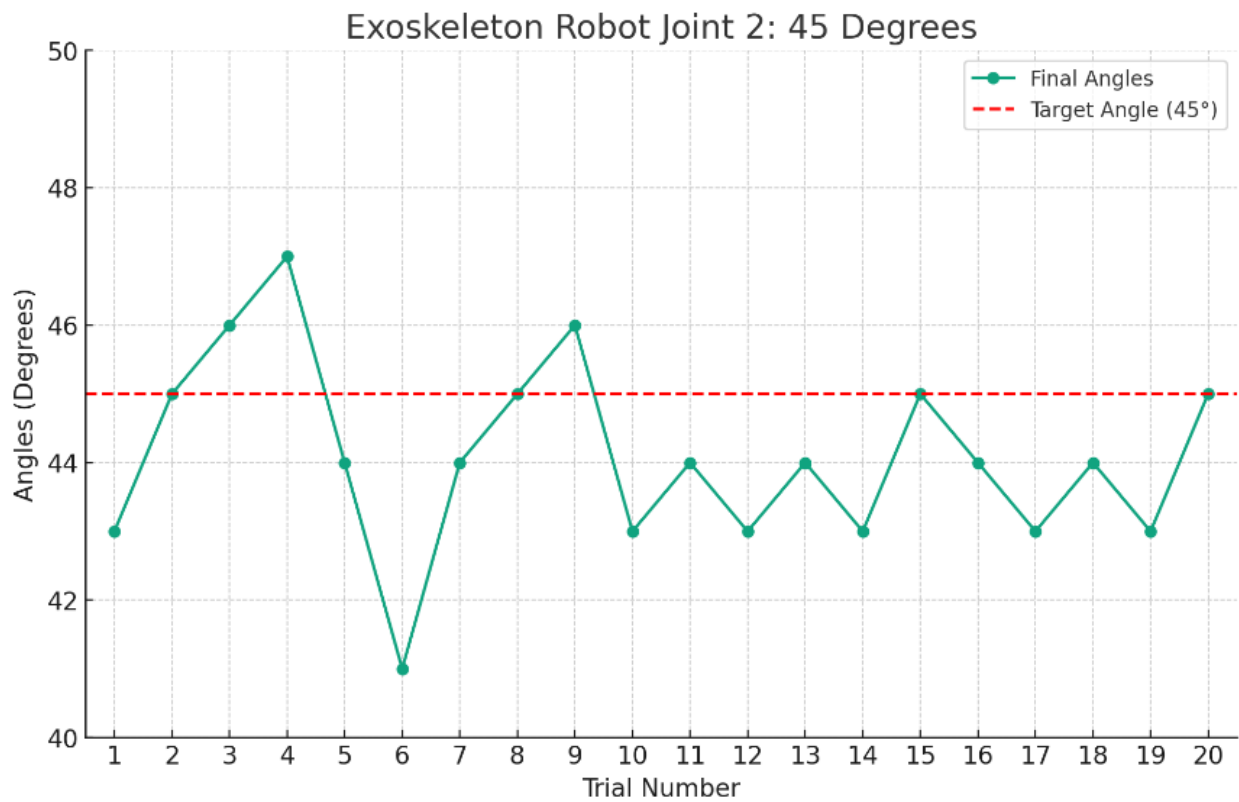


Figure 4.7

Joint 2 45 Degrees Movement Graph



In the Figure 4.7, we can evaluate that the MAE is 1.3 and RMSE is 1.61. This shows not a lot of errors when it comes to joint 2 which also has the end effector, gripper.

Figure 4.8

Joint 2 45 Degrees Movement

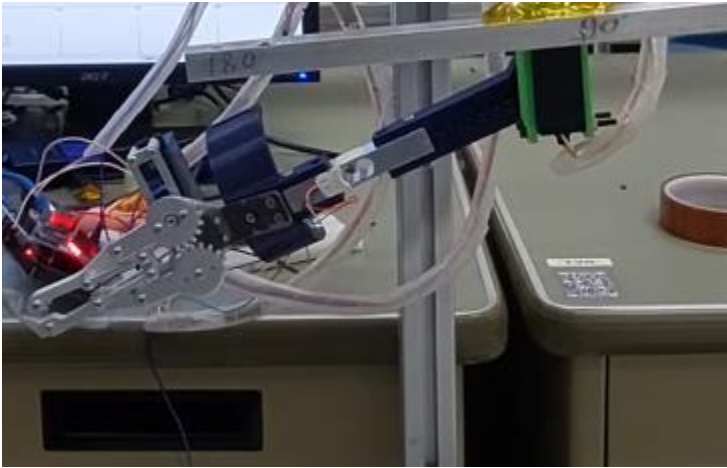
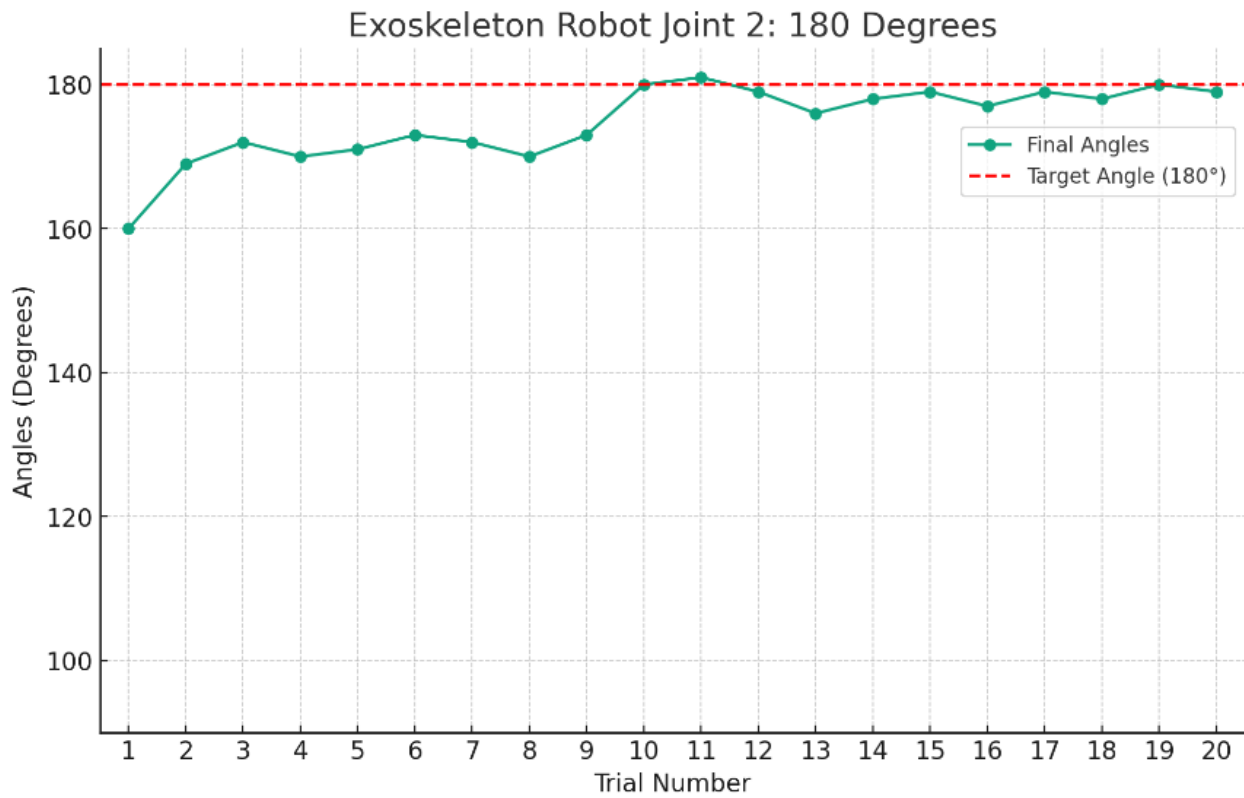


Table 4.4*Joint 2: 180 Degree Movement from 90*

Trials	Final Angles	Initial Position	Target Angle
1	160	90	180
2	169	90	180
3	172	90	180
4	170	90	180
5	171	90	180
6	173	90	180
7	172	90	180
8	170	90	180
9	173	90	180
10	180	90	180
11	181	90	180
12	179	90	180
13	176	90	180
14	178	90	180
15	179	90	180
16	177	90	180
17	179	90	180
18	178	90	180
19	180	90	180
20	179	90	180
MAE	5.3		
RMSE	7.3		

Figure 4.9

Joint 2 180 Degree from 90

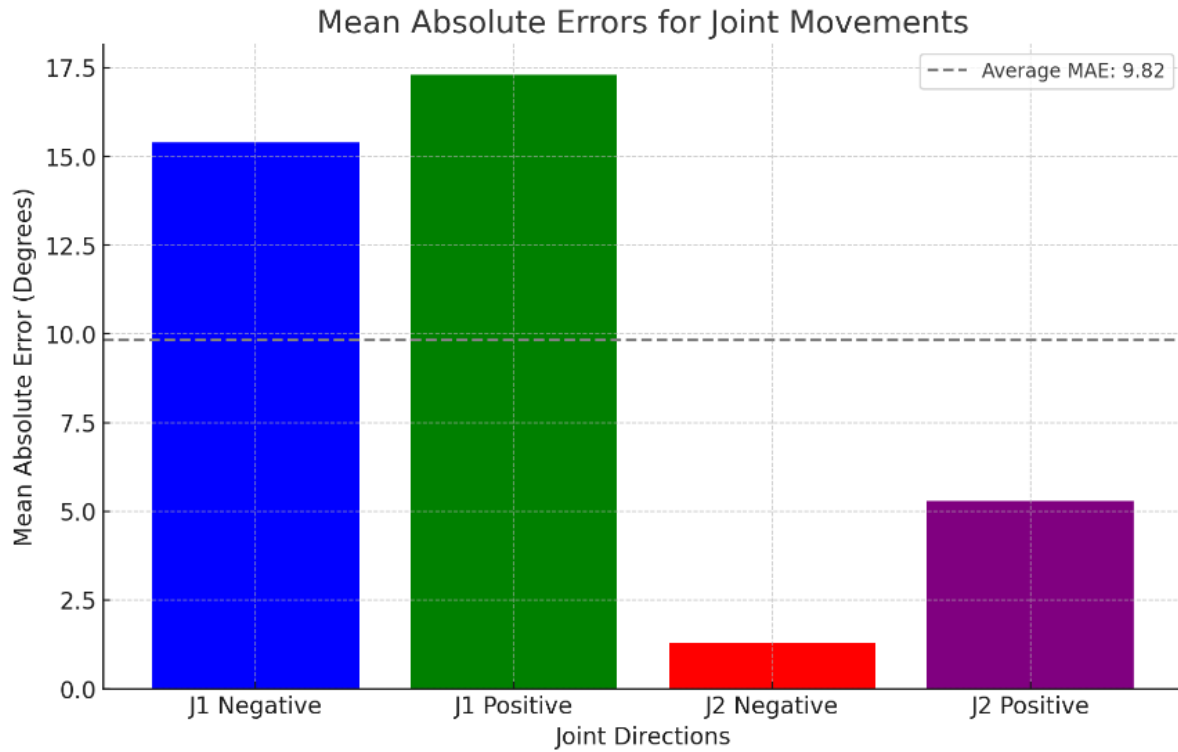


In the figure 4.9, we can see that the joint 2 of Karuna Robot reaches 180 degrees effectively at first but has difficulty in maintaining it because of perhaps lack of concentration or lesser intensity of focus. However, by the end it is able to maintain the position persistently.

We can evaluate the total Average of MAE in both the positive and negative directions in both joints of Karuna robot. In Figure 4.10, we can see the average of total MAE is about 9.82.

Figure 4.10

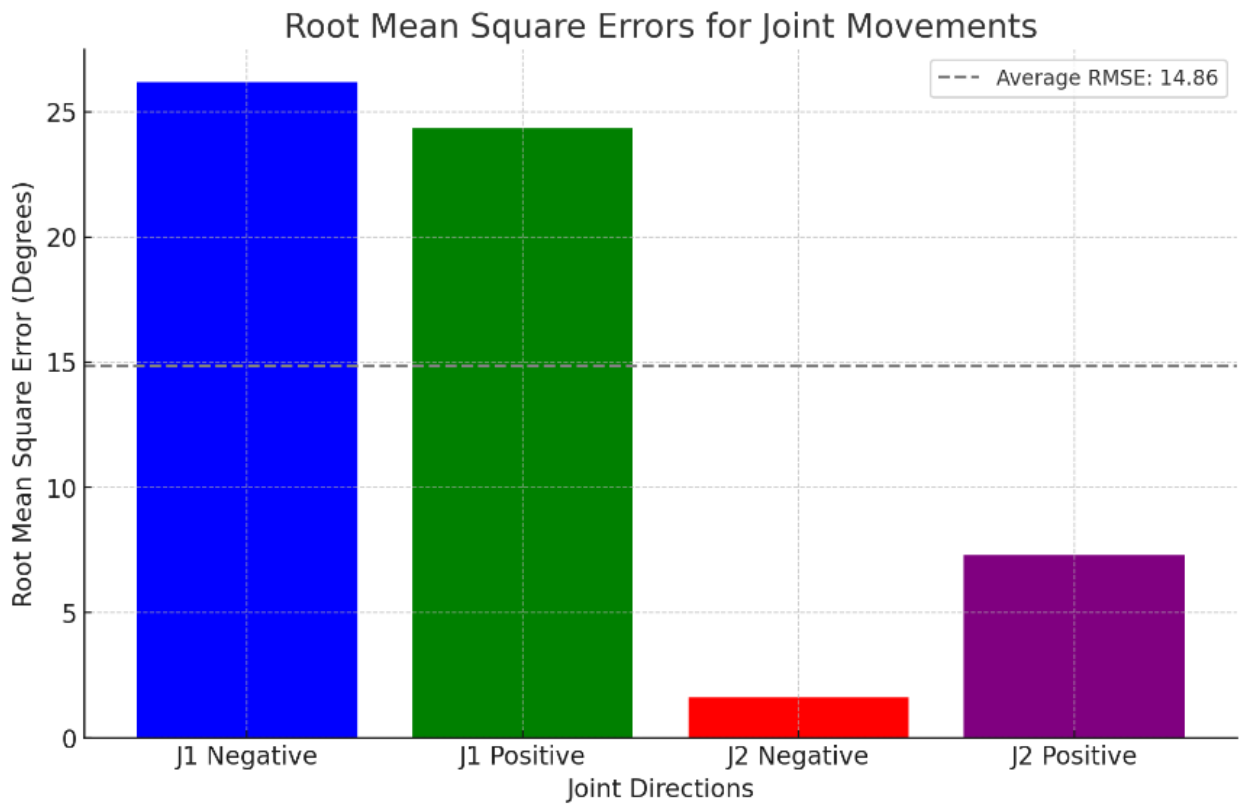
Average MAE in Both Joints.



The Average RMSE across both the joints and their direction is illustrated in Figure 4.11. It is approximately 14.86 which is significantly higher as RMSE gives the errors more weight than MAE. The higher MAE and RMSE in joint 1's both direction is prominent and it is mostly likely due to mechanical obstruction as joint 1 has more load that it needs to hold or it could also be because of lack of concentration and focus on recalling motor movement imaginations.

Figure 4.11

Average RMSE Across All Joints and Directions



4.2 Pick and Place

Karuna Robot attached in aluminum profile, with a pick and place platform in Figure 4.12.

Figure 4.12

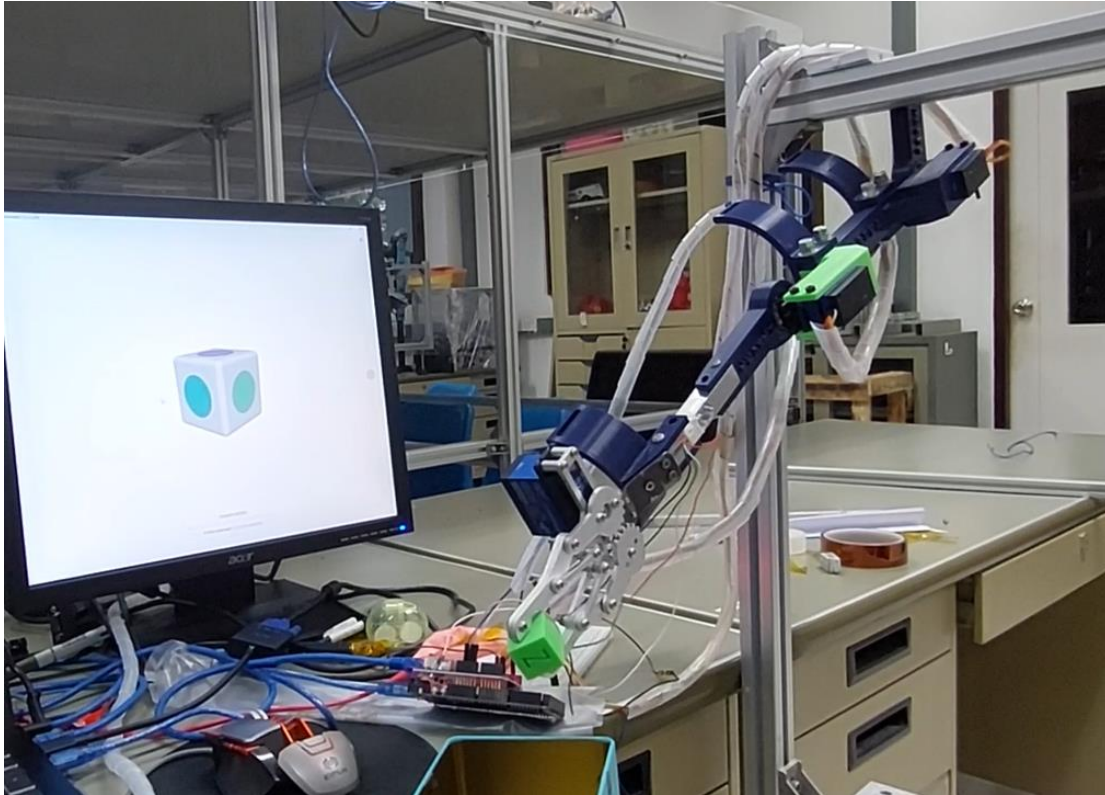
Pick and Place Set Up



The Pick place was arranged where the gripper of the robot grabs a payload (up to 75 grams without mechanical obstructions) from the plain and places it in box which is at an arm's length distance with adjustable height adjustment and the user gives mental commands which is processed using circular queue data structure and map. So even in the sequential movements, the precise placement of the end effector to depends purely on users' intensity of mental commands. The movements in the buffer of the program expects to make the pick and place will be rapidly deleted and enqueued again unless it is not receiving enough intensity of user's mental commands. Moreover, the movements also happen with the same intensity the user desires, so the success and unsuccess of pick and place will highly depend on user.

Figure 4.13

Place Operation from One point to Another



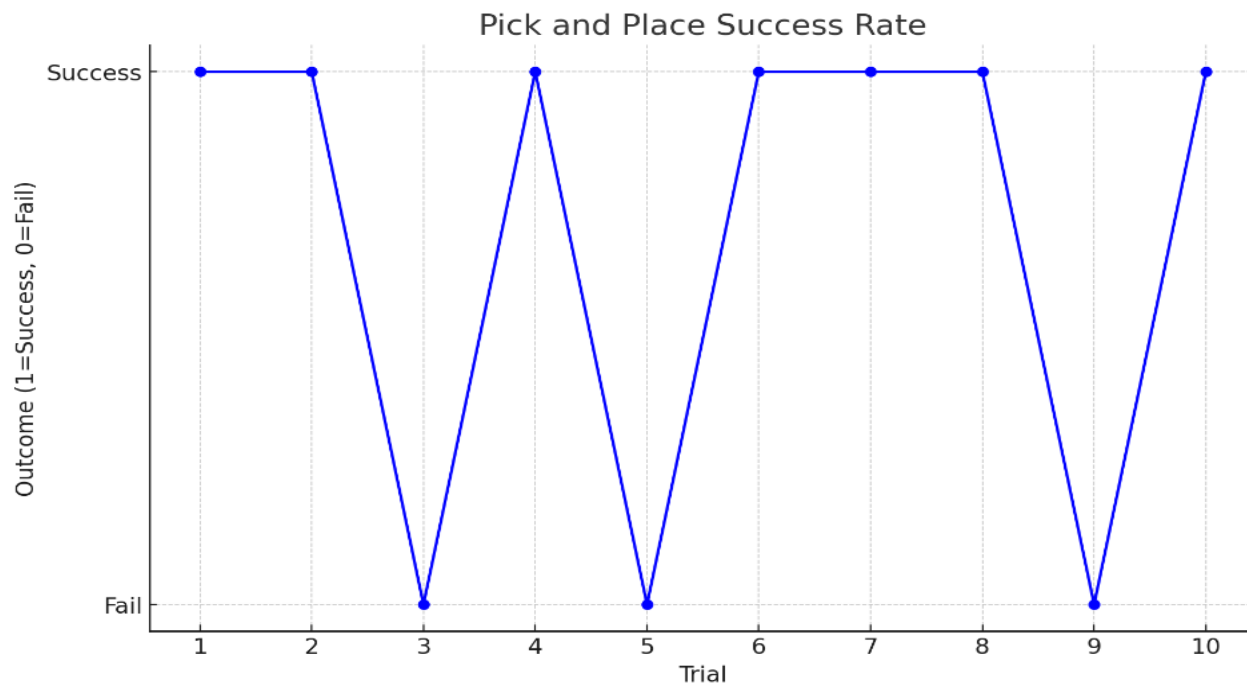
The place operation can successfully handle place once the user is able to match all the expected positive and negative movements from both joints for the robot to reach to the place phase.

Table 4.5*Ten Trials of Pick and Place*

Trial	Outcome
1	Success
2	Success
3	Unsuccess
4	Success
5	Success
6	Unsuccess
7	Success
8	Success
9	Success
10	Unsuccess
Average Success rate	70%

Figure 4.14

Pick and Place Success Rate



In the above trials each took average 2 and a half minutes to achieve but it can either be very long but can be really difficult to achieve the task in less time because it relies in the user how they are able to use mental commands.

4.3 Signals Average Band Power

The average band power of all the waves across all the electrodes were done and time stamped to derive the band power of all waves across all 5 electrodes during neutral, push, pull and lift states. The table 4.6 illustrates the band power observed in each neutral (eye blinking), push, pull, and lift mental states.

Table 4.6

Average Signal Band Power

Action	Theta	Alpha	Low Beta	High Beta
Neutral	12.0338	7.9336	1.1893	-1.2982
Push	4.6200	4.5513	-0.3526	-1.8969
Pull	6.3022	6.5420	0.7366	-0.5828
Lift	3.8988	4.4386	0.2039	-1.4720

The above recording is during a session of EEG recording during pick and place task where keystrokes q, w, e, r was pressed during the 20 seconds for each mental command were expected to be executed.

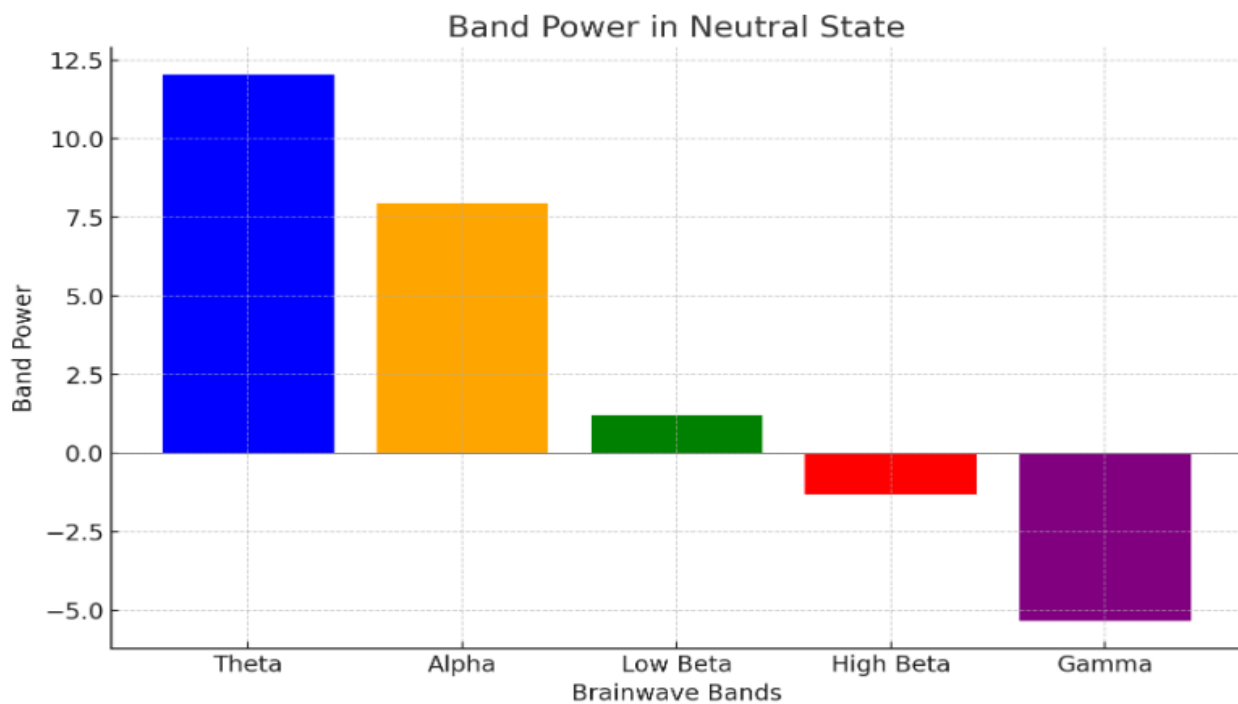
The highest Theta band is 12.0338 in neutral state indicated a relaxed or idle time, which makes sense, since we are blinking our eyes as neutral command for gripper grab command. The theta band is highest in pull command where the user recall the motor movement imagination which is more prominent in pull, other than push state with band power of 4.6200 and lift state with band power 3.8988 which is the lowest among the pure motor imaginary tasks.

It is observed that Alpha band is highest in neutral state as this is expected to occur since blinking of the eyes triggers the alpha bands the most and commonly used in other brain machine interface research. The switch from 7.9336 in neutral state to much lower 4.5513, 6.5420 and 4.4386 band power in push, pull and lift mental state shows an increase in the cognitive load and distinguishes from normal idle and relaxed state in neutral state.

The observation in low beta which is responsible for active thinking is significantly low but exists during mental commands. It is significantly low during push state with -0.3526 band power, whereas it is slightly evident in both pull and lift state with 0.7366 and 0.2039 respectively. Although, it was expected to be a little more prominent than this, it still signifies some active thinking taking place during the execution of mental commands.

Figure 4.15

Neutral State



Theta (4–7 Hz): A drop in theta band strength may indicate a change in mental state from one that is more contemplative or at ease to one that calls for more focused attention or interaction.

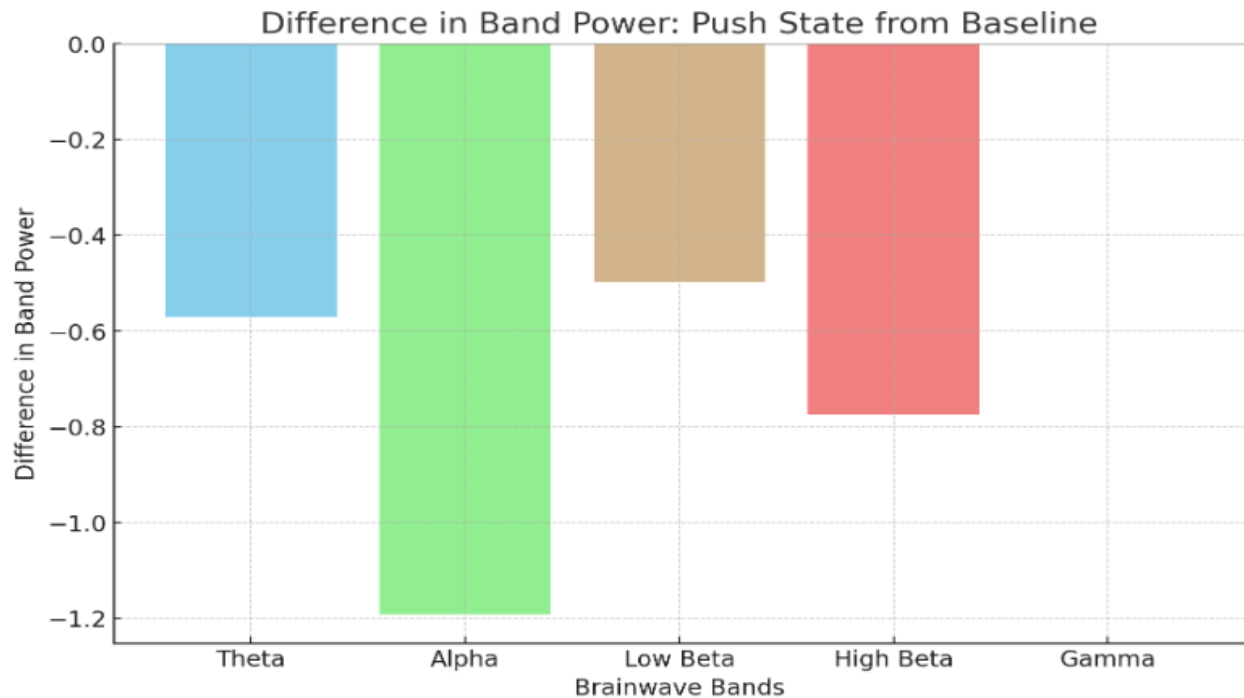
Alpha (8–13 Hz): A peaceful wakeful state is linked to alpha waves. This decrease may suggest that the brain is actively involved in cognitive or motor tasks rather than being "at rest."

Low Beta (13–16 Hz): Low beta is frequently associated with focused, active thought and busy, nervous thinking. A drop could indicate a reduction in anxiety or active involvement, even though an increase is usually expected during intense attention.

High Beta (17–30 Hz): A high degree of arousal, anxiety, or attentiveness is correlated with high beta activity.

Figure 4.16

Push State Compared with Baseline



Theta (4–7 Hz): A drop in theta band strength may indicate a change in mental state from one that is more contemplative or at ease to one that calls for more focused attention or interaction.

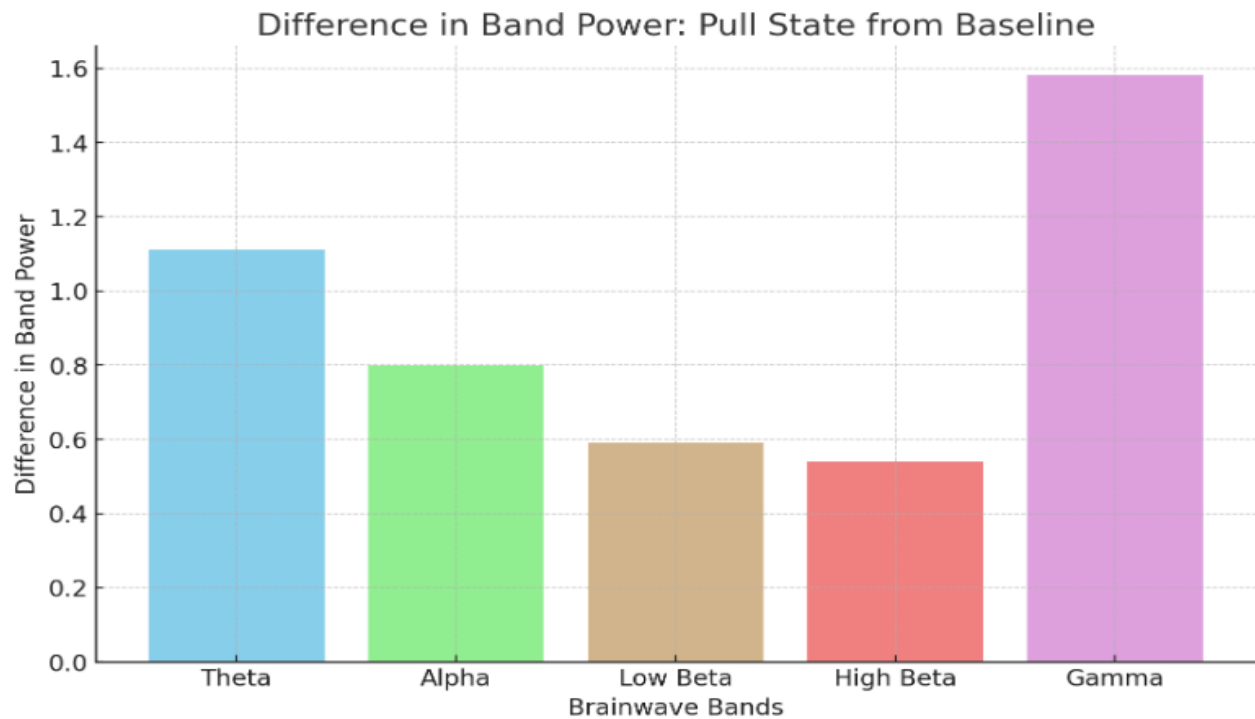
Alpha (8–13 Hz): A peaceful wakeful state is linked to alpha waves. This decrease may suggest that the brain is actively involved in cognitive or motor tasks rather than being "at rest."

Low Beta (13–16 Hz): Low beta is frequently associated with focused, active thought and busy, nervous thinking. A drop could indicate a reduction in anxiety or active involvement, even though an increase is usually expected during intense attention.

High Beta (17–30 Hz): High beta activity is linked to elevated arousal, anxiety, or awareness levels.

Figure 4.17

Pull State Compared with Baseline



Theta: An increase in relation to the baseline may indicate a shift towards a more relaxed state or greater sleepiness during the pull state.

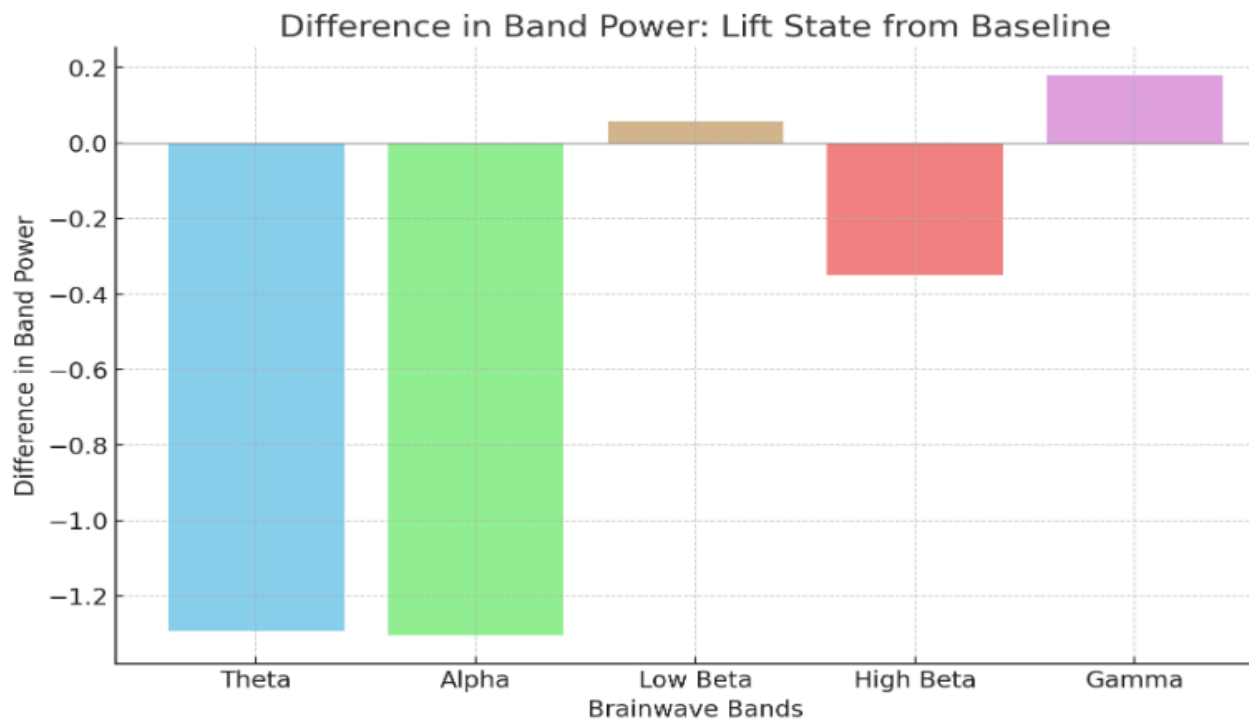
Alpha: often lowers during physical movement, an increase here typically reflects a more relaxed state, which may appear contradictory if the pull condition contains motor activity.

Low Beta: An increase is consistent with the expectation during motor activity and may indicate increased attentiveness or involvement relative to the baseline.

High Beta: A drop could mean that, in the pull state—which would be uncommon during an active motor task—stress or arousal levels were lowered.

Figure 4.18

Lift State Compared with Baseline



Theta: An increase in relation to the baseline may indicate a shift towards a more relaxed state or greater sleepiness during the pull state.

Alpha often lowers during physical movement, an increase here typically reflects a more relaxed state, which may appear contradictory if the pull condition contains motor activity.

Low Beta: An increase is consistent with the expectation during motor activity and may indicate increased attentiveness or involvement relative to the baseline.

High Beta: A drop could mean that, in the pull state—which would be uncommon during an active motor task—stress or arousal levels were lowered.

CHAPTER 5

CONCLUSION

5.1 Summary

Karuna robot with 2 DOF arm exoskeleton robot for pick and place was presented which can be moved with some degree of control based on the user's EEG signal power. It is a rehabilitation robot that tries to help people with lack of motor movements in their arm to reinstate their motor movements. There are many papers that use other techniques to use EEG signals to give commands to computer or robot but this paper tried to use motor imagery which is still in its infancy. moreover, many papers focus on improving the classification and use their algorithms to classify commands but there aren't much paper that are trying to consider the time complexity and buffering the highly variable signals from brain.

Our Data structure to handle and buffer the brain signals to filter and only use the desirable commands has made the time taken to complete pick and place task done within 2 minutes on an average. with best time complexity being $O(1)$ which means the time of execution of task is usually constant and fast. Moreover, our use of linear interpolation tries to address tasks not being just absolute positive or negative but tries to mimic the way we naturally use our hand to have only certain degree of movement as per our wish. This paper addressed the success of how our brain can recall a movement with combination of concentration and active thinking as we able to find that during mental commands, we were getting theta bands which can be understood to be recall of memory, the spike on low beta was not much but we were getting some frequency readings during the mental commands execution window which showed on active thinking or imagination which we might be able to better understand and derive in later studies.

Moreover, the presence of alpha bound from frontal lobes electrode renders planning of motor imagery. The MAE and RMSE which were higher than joint 2 indicate a possible indication that our mental command lift which was used to control the joint 1 was not much successful or needed a more replicable memory or imagination of motor movements.

5.2 Future Works

The system can be enhanced by using EEG headset with more electrodes that has Central midline or Cz, C1, C2, C3 electrodes that are responsible for better motor movements recording and analyzing. Moreover, using and creating our own classification algorithm to better recognize the patterns of mental commands can be highly useful and of scientific research purposes. Moreover, combining other Brain machine interface techniques like SSVEP and P300 might also be useful and fast when classifying tasks as they are known to be fast and easy to train as they do not depend entirely on pure motor imagination.

REFERENCES

- Benesová, M., Krivošík, M., Kosírová, S., & Foltánová, T. (2022). Secondary prevention of patients with ischaemic stroke after recanalization treatment. *European Pharmaceutical Journal*, 69(s1), 79–81. <https://doi.org/10.2478/afpuc-2022-0013>
- Pope, G. T. (1992, December 1). Power Suits. *Discover Magazine*.
<https://www.discovermagazine.com/technology/power-suits>
- Amzica, F., & Lopes da Silva, F. H. (2017). Cellular Substrates of Brain Rhythms. In D. L. Schomer & F. H. Lopes da Silva (Eds.), *Oxford Medicine Online*. Oxford University Press.
<https://doi.org/10.1093/med/9780190228484.003.0002>
- Amin, H. U., Mumtaz, W., Subhani, A. R., Saad, M. N. M., & Malik, A. S. (2017). Classification of EEG Signals Based on Pattern Recognition Approach. *Frontiers in Computational Neuroscience*, 11. <https://doi.org/10.3389/fncom.2017.00103>
- Ferris, D. P., Schlink, B. R., & Young, A. J. (2019, January 1). Robotics: Exoskeletons (R. Narayan, Ed.). *ScienceDirect;Elsevier*. <https://www.sciencedirect.com/science/article/abs/pii/B9780128012383999069>
- Esposito, D., Centracchio, J., Andreozzi, E., Gargiulo, G. D., Naik, G. R., & Bifulco, P. (2021). Biosignal-Based Human–Machine Interfaces for Assistance and Rehabilitation: A Survey. *Sensors*, 21(20), 6863. <https://doi.org/10.3390/s21206863>
- Musk, E. (2019). An Integrated Brain-Machine Interface Platform With Thousands of Channels (Preprint). *Journal of Medical Internet Research*, 21(10). <https://doi.org/10.2196/16194>
- Volker Bartenbach , (2017). Exoskeleton | EduExo. (2023). Auxivo. Retrieved September 18, 2023, from <https://www.auxivo.com/eduexo>
- bin Imtiaz, M. S., Babar Ali, C., Kausar, Z., Shah, S. Y., Shah, S. A., Ahmad, J., Imran, M. A., & Abbasi, Q. H. (2021). Design of Portable Exoskeleton Forearm for Rehabilitation of Monoparesis Patients Using Tendon Flexion Sensing Mechanism for Health Care Applications. *Electronics*, 10(11), 1279. <https://doi.org/10.3390/electronics10111279>
- Bhagat, N. A., French, J., Venkatakrishnan, A., Yozbatiran, N., Francisco, G. E., O'Malley, M. K., & Contreras-Vidal, J. L. (2016, March 31). Design and Optimization of an EEG-Based

- Brain Machine Interface (BMI) to an Upper-Limb Exoskeleton for Stroke Survivors. *Frontiers in neuroscience*, 10, 122. <https://doi.org/10.3389/fnins.2016.00122>
- Xu, B., Song, A., Zhao, G., Xu, G., Pan, L., Yang, R., Li, H., Cui, J., & Zeng, H. (2015). Robotic neurorehabilitation system design for stroke patients. *Advances in Mechanical Engineering*, 7(3), 168781401557376. <https://doi.org/10.1177/1687814015573768>
- Paredes-Acuna, N., Berberich, N., Dean-Leon, E., & Cheng, G. (2022). Tactile-based assistive method to support physical therapy routines in a lightweight upper-limb exoskeleton. *IEEE Transactions on Medical Robotics and Bionics*, 4(3), 541-549. <https://doi.org/10.1109/TMRB.2022.3188429>
- Missiroli, F., Lotti, N., Xiloyannis, M., Sloom, L. H., Riener, R., & Masia, L. (2020). Relationship between muscular activity and assistance magnitude for a myoelectric model based controlled exosuit. *Frontiers in Robotics and AI*, 7, 595844. <https://doi.org/10.3389/frobt.2020.595844>
- Emotiv .(2023). Insight 2 [EMOTIV Insight 2.0 – 5 Channel Mobile Brainwear]. <https://www.emotiv.com/product/emotiv-insight-5-channel-mobile-brainwear/>
- Xiao, Z. G., Elnady, A. M., Webb, J., & Menon, C. (2014, August). Towards a brain computer interface driven exoskeleton for upper extremity rehabilitation. In 5th IEEE RAS/EMBS international conference on biomedical robotics and biomechatronics (pp. 432-437). IEEE.
- Saiful. (2023, April 27). Bowden Cable: The Surprising Technology Behind Smooth Mechanical Operations. *Aerospaceer*. <https://aerospaceer.com/bowden-cable/>
- Wei, W., Qu, Z., Wang, W., Zhang, P., & Hao, F. (2018). Design on the bowden cable-driven upper limb soft exoskeleton. *Applied bionics and biomechanics*. <https://doi.org/10.1155/2018/1925694>
- Samper-Escudero, J. L., Gimenez-Fernandez, A., Sánchez-Urán, M. Á., & Ferre, M. (2020). A cable-driven exosuit for upper limb flexion based on fibres compliance. *IEEE Access*, 8, 153297-153310. <https://doi.org/10.1109/ACCESS.2020.3018418>
- Kang, H. B., & Wang, J. H. (2013). Adaptive control of 5 DOF upper-limb exoskeleton robot with improved safety. *ISA transactions*, 52(6), 844-852. <https://doi.org/10.1016/j.isatra.2013.05.003>
- Abe, T., Koizumi, S., Nabae, H., Endo, G., Suzumori, K., Sato, N., ... & Takamizawa, F. (2019). Fabrication of “18 weave” muscles and their application to soft power support suit for

- upper limbs using thin mckibben muscle. *IEEE Robotics and Automation Letters*, 4(3), 2532-2538.
- Kim, W. S., Lee, H. D., Lim, D. H., Han, J. S., Shin, K. S., & Han, C. S. (2014). Development of a muscle circumference sensor to estimate torque of the human elbow joint. *Sensors and Actuators A: Physical*, 208, 95-103. <https://doi.org/10.1016/j.sna.2013.12.036>
- Da Silva, L. D., Pereira, T. F., Leithardt, V. R., Seman, L. O., & Zeferino, C. A. (2020). Hybrid impedance-admittance control for upper limb exoskeleton using electromyography. *Applied Sciences*, 10(20), 7146. <https://doi.org/10.3390/app10207146>
- AJ Martínez - Mata, Andrés Blanco Ortega, Guzmán - Valdivia, C. H., A. Abundez - Pliego, GarcíaVelarde, M., Andrea Magadán Salazar, & Osorio, R. (2023). Engineering design strategies for force augmentation exoskeletons: A general review. *International Journal of Advanced Robotic Systems*, 20(1), 172988062211494-172988062211494. <https://doi.org/10.1177/17298806221149473>
- Xu, B., Song, A., Zhao, G., Xu, G., Pan, L., Yang, R., Li, H., Cui, J., & Zeng, H. (2015). Robotic neurorehabilitation system design for stroke patients. *Advances in Mechanical Engineering*, 7(3), 168781401557376. <https://doi.org/10.1177/1687814015573768>